Check for updates

Received: 25 September 2023 | Accepted: 20 November 2023

DOI: 10.1002/bem.22495

RESEARCH ARTICLE

BioEM WILEY

Evaluation of mitochondrial stress following ultraviolet radiation and 5G radiofrequency field exposure in human skin cells

Lorenza Patrignoni PhD[1] | **Annabelle Hurtier**[2] | **Rosa Orlacchio**[1] | **Alexandre Joushomme PhD**[2] | **Florence Poulletier de Gannes**[2] | **Philippe Lévêque RD**[3] | **Delia Arnaud-Cormos**[3] | **Hamid Reza Revzani RD**[4] | **Walid Mahfouf**[4] | **André Garenne**[2] | **Yann Percherancier RD**[2] | **Isabelle Lagroye**[1]

[1]Paris Sciences et Lettres Research University-École Pratique des Hautes Études (EPHE), IMS laboratory - SANE team, Paris, France

[2]Univ. Bordeaux, CNRS, IMS laboratory / UMR 5218, SANE Team, Talence, France

[3]Univ. Limoges, CNRS, XLIM / UMR 7252, RF-ELITE team, Limoges, France

[4]Univ. Bordeaux, Inserm, BRIC / UMR 1312, TRIO2 team, Bordeaux, France

Correspondence

Isabelle Lagroye, Paris Sciences et Lettres Research University-École Pratique des Hautes Études (EPHE), F-75006 Paris, France.
Email: isabelle.lagroye@ephe.psl.eu

Funding information

ANSES, Grant/Award Number: 2019/2RF/018; New Aquitaine regional council, Grant/Award Number: AAPR2020A-2019-8140010

Abstract

Whether human cells are impacted by environmental electromagnetic fields (EMF) is still a matter of debate. With the deployment of the fifth generation (5G) of mobile communication technologies, the carrier frequency is increasing and the human skin becomes the main biological target. Here, we evaluated the impact of 5G-modulated 3.5 GHz radiofrequency (RF) EMF on mitochondrial stress in human fibroblasts and keratinocytes that were exposed for 24 h at specific absorption rate of 0.25, 1, and 4 W/kg. We assessed cell viability, mitochondrial reactive oxygen species (ROS) production, and membrane polarization. Knowing that human skin is the main target of environmental ultraviolet (UV), using the same read-out, we investigated whether subsequent exposure to 5G signal could alter the capacity of UV-B to damage skin cells. We found a statistically significant reduction in mitochondrial ROS concentration in fibroblasts exposed to 5G signal at 1 W/kg. On the contrary, the RF exposure slightly but statistically significantly enhanced the effects of UV-B radiation specifically in keratinocytes at 0.25 and 1 W/kg. No effect was found on mitochondrial membrane potential or apoptosis in any cell types or exposure conditions suggesting that the type and amplitude of the observed effects are very punctual.

KEYWORDS

5G, mitochondria, radiofrequency, reactive oxygen species, skin

1 | INTRODUCTION

Radiofrequency (RF) electromagnetic fields (EMF) are part of the electromagnetic spectrum ranging from 100 kHz to 300 GHz. They encompass frequencies exhibiting electric and magnetic properties and are considered nonionizing, meaning that they lack the energy required to disrupt atoms and molecules via ionization. Currently, the fifth generation (5G) technology is being deployed to provide higher data and faster response rates. It will combine new allocated frequency bands at 3.5 and 26 GHz in addition to those already used for 2G, 3G, and 4G. The first band, commonly referred as the C-band, is a crucial component of the current 5G infrastructure because it strikes a balance between providing extensive broadband coverage and fast speeds. At the other end of the spectrum considered, the 26 GHz band has limited ability to penetrate buildings and propagate signals efficiently, making it more suitable for covering specific areas with high data traffic. In addition, the 3.5 GHz band can utilize the same cell sites as the current antennas. With the growing deployment of wireless communication signals, the populations are thus exposed to new environmental

RF-EMF. As for previous signal generations, 5G deployment raises questions about the potential harmful effects on human health. Since the advent of the 2G, including the Global System for Mobile (GSM) signals, the scientific community has had a better understanding of the interaction of RF waves with living matter. After more than 20 years of active research, the thermal effect remains the only established interaction mechanism. While a huge number of studies have investigated the existence of nonthermal effects under RF-EMF exposure in different models (i.e., cells, animals, humans) in the existing frequency bands for mobile communications, no conclusive evidence for such effects was reached (ICNIRP 2020). To protect the population from thermal adverse health effects of RF-EMF exposure, including 5G signals, the International Commission on Non-Ionizing Radiation Protection (ICNIRP) has set exposure limits (International Commission on Non-Ionizing Radiation Protection, 1998; ICNIRP, 2020).

To our knowledge, only a few published articles have examined the effects of 5G technology in experimental studies (EMF-Portal, 2022) at the specific band of 3.5 GHz. Among these, the exposure of zebrafish embryos at specific absorption rate (SAR) of 8.27 W/kg induced depressed sensorimotor function, abnormal behavioral responses, and variations in the expression of genes related to metabolic function in adult zebrafish (Dasgupta et al., 2020, 2022). In *Drosophila melanogaster*, 3.5 GHz exposure enhanced the expression of heat shock, oxidative stress, and humoral immunity system genes leading to fly developmental promotion (Wang et al., 2022). In addition, long-term exposure resulted in alterations of the expression of circadian clock genes resulting in improvement of sleep duration (Wang et al., 2021). Exposure of diabetic and healthy rats brains revealed an increase in appetite, energy metabolism, and oxidative stress (Bektas et al., 2022). Finally, no effect on anxiety-like behavior, but a SAR-dependent increase in different oxidative stress parameters were found in the guinea pig auditory cortex (Yang et al., 2022). Unfortunately, all these studies are highly heterogeneous in terms of endpoints, biological systems, and SAR levels, making it impossible to draw firm conclusions about the effects of 3.5 GHz signals on human health. It is also essential to indicate that all these studies used either an unmodulated or a GSM-modulated 3.5 GHz signal, but none of them used a 5G-modulated signal. In addition, none of the above-mentioned studies addressed the skin or other superficial tissues as relevant targets. Actually, since the penetration of the RF-EMF into the tissues decreases as the frequency increases, and given the large amount of water in the skin (Christ et al., 2006; Feldman et al., 2009), this tissue is susceptible to absorb most of the RF-EMF power when exposed to the 5G highest frequency ranges, that is, at 3.5 GHz and even more at 26 GHz.

Highlights

- A 24 h exposure to a 5G signal at 3.5 GHz was able to statistically significantly alter the mitochondrial reactive oxygen species (ROS) production in human skin fibroblasts (decrease at 1 W/Kg) and in human keratinocytes after UV-B irradiation (increase at 0.25 and 1 W/kg).
- A 24 h exposure to a 5G signal at 3.5 GHz was not able to alter cell viability, apoptosis and mitochondrial membrane potential in human skin cells, either alone or after UV-B irradiation.
- Further studies on 3D or in vivo skin models would be needed to conclude about a possible effect of 5G 3.5 GHz signal on ROS production.

The skin is not only the largest but also the most prominent organ in the human body. Its primary function is to provide a protective barrier against external stimuli. The skin comprises three distinct layers: the epidermis, the dermis, and the hypodermis. The outermost layer, the epidermis, is between 0.05 and 1.5 mm thick and is primarily composed of keratinocytes, which exist in various states of differentiation. Additionally, it contains other specialized cells such as melanocytes, Merkel cells, and Langerhans cells. The second layer, the dermis, is much thicker, ranging from 1 to 5 mm, and provides support to the epidermis while also connecting it to the hypodermis. The dermis comprises a complex network of connective tissues, including fibroblasts, macrophages, plasma cells, mast cells, as well as various nerves, hair follicles, sweat glands, lymphatic, and blood vessels. Finally, the hypodermis is the deepest layer and is primarily composed of adipocytes that serve as energy and heat supplies, in addition to connective tissue. This layer acts as a bridge that connects the skin to the underlying fibrous tissue of the bones and muscles, providing support and stability to the skin (Kolarsick et al., 2011; Lawton, 2019).

In addition to RF-EMF, other environmental physical agents, that is, ultraviolet radiations (UV-R) are known to target the skin. Small amounts of UV-R are known to be beneficial to health and play an essential role in the synthesis of vitamin D. However, over-exposure is clearly associated with DNA mutagenicity, apoptosis, and cutaneous melanoma (Kraemer, 1997). Based on extensive epidemiological and experimental studies, UV-R was classified as Class I human carcinogen by IARC (A Review of Human Carcinogens, 2012). Depending on the

1521186x, 2024, 3, Downloaded from https://onlinelibrary.wiley.com/doi/10.1002/bem.22495 by University Of British Columbia, Wiley Online Library on [10/10/2026]. See the Terms and Conditions (https://onlinelibrary.wiley.com/terms-and-conditions) on Wiley Online Library for rules of use; OA articles are governed by the applicable Creative Commons License

wavelength, UV-R can be divided into UV-A (315–400 nm), UV-B (280–315 nm), and UV-C (100–280 nm). UV-A which represent approximately 95% of the UV sun's rays reaching the earth's surface, bring the lowest energy and can penetrate deep into the dermis acting as an initiator of aging (Krutmann, 2001). On the other hand, UV-B radiations mainly impact epidermis, causing sunburn. UV-B radiations are directly absorbed by the DNA, resulting in more cytotoxic and mutagenic effects than UV-A. The most common UV mutations, also called "UV signature," consists in base substitutions at dipyrimidine sites. Such substitutions lead to specific DNA photoproducts as cyclobutane pyrimidine dimers (CPDs) and pyrimidine (6–4) pyrimidone (Ikehata & Ono, 2011). In addition, both UV-B and UV-A are responsible for reactive oxygen species (ROS) production that may lead to indirect DNA damage and apoptosis (Heck et al., 2003; Sander et al., 2004).

Several recent studies suggested that RF-EMF in the GHz range may trigger oxidative stress in exposed cells or animals (Schuermann & Mevissen, 2021; Yakymenko et al., 2016). This is even more important since excessive, unbalanced levels of ROS can interfere with many cellular processes and functions. If the original situation is not restored, excessive ROS production can affect the onset and progression of many diseases, such as cancer, diabetes, or neurodegenerative syndromes (Brieger et al., 2012; Sies et al., 2017). Hence, it appears mandatory to determine whether exposure to 5G-modulated signals in the new frequency band of 3.5 GHz could affect living systems.

In the present study, we aimed at investigating the impact of a 24 h 5G-modulated 3.5 GHz signal on skin cells, at three different SAR: 0.25, 1, and 4 W/kg. For this purpose, we used human Xp6be fibroblasts and KHAT keratinocytes, that were pre-exposed or not to UV-B, and we measured mitochondrial ROS generation and change in the mitochondrial membrane potential ($\Delta\Psi_m$), as well as cellular apoptosis and necrosis.

2 | MATERIALS AND METHODS

2.1 | Cell Lines

For our experiments, we used human-immortalized skin fibroblasts (Xp6be) (Coriell Institute) (Moisan et al., 2012) and the KHAT cell line of keratinocytes. To obtain this latter, primary keratinocytes were isolated from surgical excision biopsies of patients who had previously signed a non-opposition agreement for the use of cells for research purposes (Declaration of Helsinki). The cells were grown in Keratinocyte serum-free medium (KSFM) supplemented with 50 µg/mL of bovine pituitary extract and 0.5 ng/mL of epidermal growth factor (Gibco; Thermo Fisher Scientific) in a humidified atmosphere of 5% CO_2 at 37°C. Immortalization of human primary keratinocytes were performed through their transduction with lentiviral vector expressing hTERT and the large tumor antigen (also called large T-antigen). Transduced keratinocytes were cultivated in parallel with the nontransduced cells in KSFM. Immortalization has been considered to be occurred when KHAT cells grew for 50 population doublings beyond the life span of the parental keratinocytes. These immortalized cells formed a normally stratified epidermis when used in organotypic culture (personal communication).

Xp6be fibroblasts were maintained in Dulbecco's Modified Eagle Medium composed of Nutrient Mixture F-12 (DMEM/F-12) supplemented with 10% fetal bovine serum and 1% penicillin-streptomycin (Thermo Fisher Scientific).

KHAT cells were cultured in KSFM supplemented with 5 µg/mL of Gentamicin (Gibco™; Thermo Fischer Scientific), 25 mg of Bovine Pituitary Extract, and 2.5 µg of human recombinant Epidermal Growth Factor (rEGF) (Gibco™; Thermo Fisher Scientific).

Both cell types were grown up to 80% confluence in plastic flasks at 37°C in a humidified atmosphere containing 5% CO_2. Subconfluent cells were harvested with a *Trypsin-EDTA* 0.05% solution (Sigma Chemical Co.) and placed in separate six-well plates, one for each experimental protocol. Twenty-four hours after the seeding, cells underwent UV-B and/or RF-EMF exposure. Meanwhile, each control group was subjected to the same procedure and timing as its corresponding exposure group but in absence of treatment. Using this setup, we prepared all cultures from the same batch with the aim of reducing the possible variability that might be caused by differences between batches and in the cell cycle.

After 24 h of RF-EMF exposure, the flow cytometry assays were performed.

2.2 | Exposure system and dosimetry

2.2.1 | Exposure to UV-B radiation

UV-B irradiation was delivered using a Bio-Link® BLX-E312 equipment (Vilber Lourmat; Fisher Bioblock), at the specific wavelength of 312 nm. Before irradiation, the dose was checked using a calibrated radiometer X9-6 (Gigahertz Optik GmbH).

Following a toxicological approach, we plotted dose-response curves for UV-B irradiation for each skin cell type and each biological outcome. Therefore, we chose the UV-B dose that induced about 50% of the maximal effect (Table 1). This procedure allowed us to detect whether a 5G modulated-3.5 GHz signal could impact, that is, increase or decrease the effect of UV-B irradiation on skin cells.

1521186x, 2024, 3, Downloaded from https://onlinelibrary.wiley.com/doi/10.1002/bem.22495 by University Of British Columbia, Wiley Online Library on [10/10/2026]. See the Terms and Conditions (https://onlinelibrary.wiley.com/terms-and-conditions) on Wiley Online Library for rules of use; OA articles are governed by the applicable Creative Commons License

TABLE 1 UV-B doses used for the experiments depending on the cell type and the biological parameter tested.

	Cell line	
Biological parameter	**Xp6be**	**KHAT**
ROS induction	5.08 ± 0.63 mJ/cm²	16.4 ± 1.03 mJ/cm²
Membrane depolarization	30.6 ± 0.11 mJ/cm²	43.93 ± 0.4 mJ/cm²

Abbreviation: ROS, reactive oxygen species.

During UV-B irradiation, the medium was replaced with phosphate-buffered saline (PBS), to avoid photoactive compounds formation. Immediately after, cells were placed in fresh medium for 24 h without exposure, or under RF-EMF exposure, in the case of consecutive exposures (Figure 1). Irradiation time to UV-B is dose-dependent but it is less than one minute at the highest dose of 43.93 mJ/cm^2. The control group, named "Mock UVB", was prepared and kept under the same condition as the irradiated sample but without any UV-B irradiation.

2.2.2 | RF-EMF setup and dosimetry

Exposure of cells to 5G-modulated signals at 3.5 GHz was performed using an innovative reverberation chamber (RC) (Orlacchio et al., 2023), that is, an electrically large cavity made of metallic walls where a homogeneous field distribution was achieved through random mechanical stirring of the field components (Hill, 1998). This is particularly convenient in bioelectromagnetic experiments to ensure a highly homogeneous exposure level regardless of the samples location within the exposure system (Capstick et al., 2017; Ito & Bassett, 1983). In this study, a cell culture incubator (150 L; BINDER Gmbh), was converted into an RC to guarantee 24 h in vitro exposure under controlled biological conditions (37°C, 5% CO_2, and 95% humidity). A detailed description of the system schematically represented in Figure 1a was given in (Orlacchio et al., 2023). The main components are reported hereafter. A printed patch antenna was used to deliver 5G-modulated 3.5 GHz signal in the chamber. A metallic stirrer composed of eight rectangular blades ($8 \times 10 \times 1$ cm^3) was mounted on a 30 cm mast to continuously rotate through a motorized precision rotation stage (PRM1/MZ8; Thorlabs Inc.) driven via a K-Cube dc servo controller (KDC101; Thorlabs). The continuous rotation modified the boundary conditions during exposure allowing to achieve a homogeneous and isotropic averaged EMF within the samples (Serra et al., 2017). A plastic holder with five shelves was used to accommodate 6- and 96-well tissue culture plates

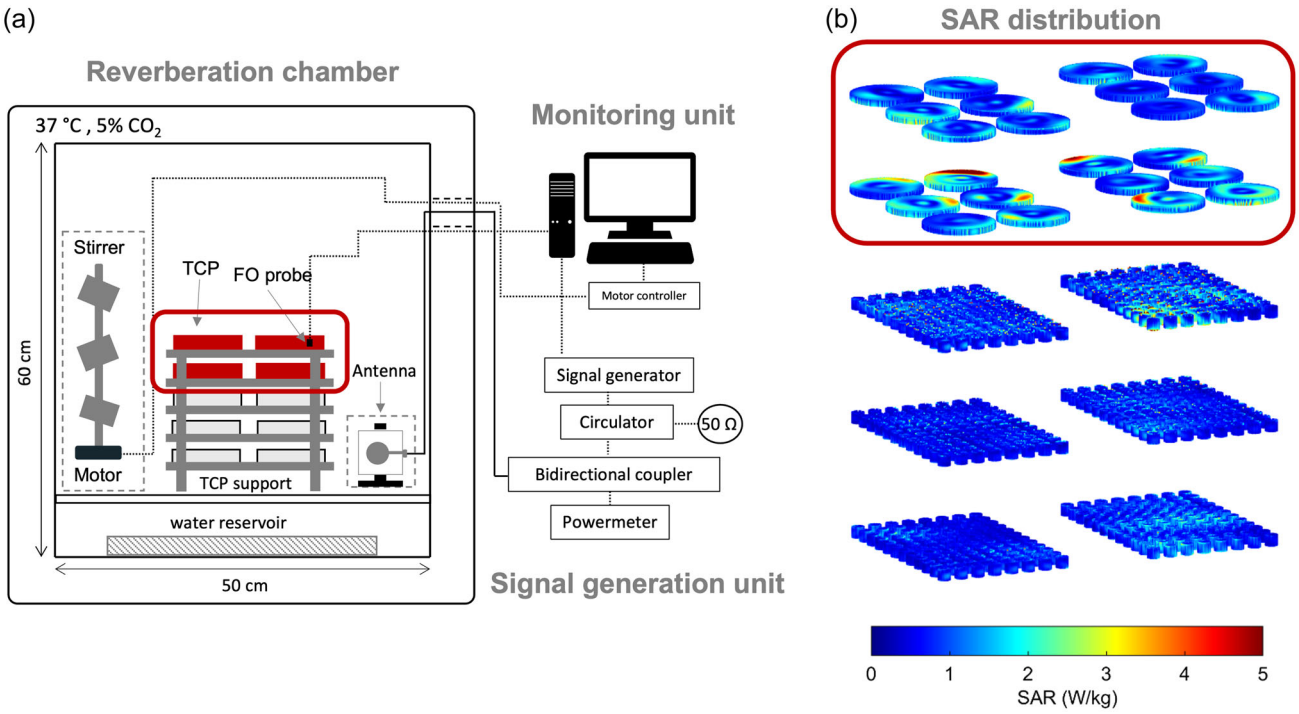


FIGURE 1 Exposure setup and specific absorption rate (SAR) distribution in the exposed samples. (a) Schematic of the exposure setup used for cellular experiments under 5G-modulated signals at 3.5 GHz. (1) The cell culture incubator converted into a reverberation chamber containing the patch antenna, the stirrer with its motor, the plastic support accommodating 10 tissue culture plates (TCPs), the fiber optic (FO) probe used for temperature measurements, and the water reservoir. Six-well TCPs used for cellular exposure are shown in red, while 96-well TCPs needed to guarantee the desired exposure level are shown in gray; (2) Signal generation unit; and (3) Monitoring unit. (b) Six-well TCPs SAR distributions normalized to 1 W incident power.

15231186x, 2024, 3, Downloaded from https://onlinelibrary.wiley.com/doi/10.1002/bem.22495 by University Of British Columbia, Wiley Online Library on [10/10/2026]. See the Terms and Conditions (https://onlinelibrary.wiley.com/terms-and-conditions) on Wiley Online Library for rules of use; OA articles are governed by the applicable Creative Commons License

(TCPs). For exposure, the chamber was loaded with 10 TCPs, including four six-well TCPs located on the two top levels of the holder (red TCPs in Figure 1a) and six 96-well TCPs set on the three bottom levels (gray TCPs in Figure 1a). Each well of the 6- and 96-well TCPs was filled with 2 ml and 200 µl of cell culture medium, respectively. A water reservoir located at the bottom of the incubator provided the desired humidity level. A metallic grid was used to sustain the antenna, the stirrer with its rotation stage, and the TCPs holder. To ensure statistical field uniformity and isotropy, the components were set at a distance greater than $\lambda/4$ and $\lambda/2$ from each other and from the incubator walls, respectively, with λ the free space wavelength at 3.5 GHz equal to 8.5 cm (Hill, 2005). The signal generation unit, located outside the cell culture incubator, was composed of an RF signal generator (SMBV100A; Rohde & Schwarz), a 45-dB gain amplifier (Mini-circuits, ZHL-16W-43+), a power circulator (Pasternack, PE83CR1005), a bidirectional coupler (Mini-circuits, ZGBDC30-372HP+), and a power meter (Agilent N1912A). The 3.5-GHz 5G signal used corresponds to 5G NR (release 15, Digital Standards SMBVB-K444; Rohde & Schwarz) with FDD duplexing, QPSK modulation, and 100 MHz channel bandwidth. Monitoring of the exposure parameters, including duration, input power, and stirrer rotation, was performed using MATLAB (The MathWorks, Inc.).

The performances of the exposure system as an RC were characterized in detail through a fast and precise technique based on the measurements of the S_{11} scattering parameters of the emitting antenna for N stepwise mode stirrer positions and different chamber configurations (Hill, 2005). In addition, accurate experimental and numerical dosimetry, that is, the quantification of the absorbed dose in biological samples exposed to electromagnetic waves was precisely performed. SAR, defined as the electromagnetic power dissipated per unit mass in the exposed sample [W/kg] was used as a metric to quantify the exposure level. Local SAR at the cellular level within an approximate volume of 1 mm^3 was experimentally retrieved from the electromagnetic-induced heating recorded with a fiber-optic thermometer (Luxtron One; Lumasense Technologies) (Nefzi, 2021; Orlacchio et al., 2023). To validate experimental local SAR values and access SAR distribution in all the exposed samples, numerical simulations using finite difference time domain (FDTD)-based electromagnetic methodology (Leveque et al., 1992; Orlacchio et al., 2023) were also performed.

To achieve the biological requirements of this study, cells were exposed in four six-well TCPs located on the holder top two levels. However, for experiments, the incubator was loaded with the same configuration used for the electromagnetic characterization, that is, four six-well and six 96-well TCPs, respectively. Indeed, SAR values may widely vary as a function of the losses in the RC which depend on the quantity of culture medium used to cover cell monolayers (Orlacchio et al., 2023).

The average local SAR, extracted from temperature measurements at the bottom of the six-well TCPs, where cells are located during exposure, was around 1.5 W/kg per 1 W of incident power with a maximum variation between different locations of the wells <30%. Numerical local SAR was consistent with experimental measurements with standard deviation of less than 30%. SAR spatial distribution normalized to 1 W incident power in the whole volume of the six TCPs is reported in Figure 1b. Overall, numerical SAR shows a good homogeneity with differences in the exposed samples within 30% that remain consistent with guidelines for accurate bioelectromagnetic exposures (ICNIRP, 2020). According to measured and simulated SAR values, the antenna input power was tuned to obtain required exposure levels of 0.25, 1, and 4 W/kg in the exposed six-well TCPs.

The temperature increase underexposure was verified using a fiber-optic probe (Luxtron) placed on the bottom of the well, in the vertical position, within the culture medium. The temperature rise was assessed by at least three measurements, and it was compensated by setting the incubator temperature to obtain 37°C during the exposure. The maximum temperature increase was about 2.03 ± 0.08°C, measured when using the highest SAR level, that is, 4 W/kg.

2.2.3 | Experimental protocol

On the day after seeding, cells were exposed or sham-exposed to different stressors as shown in Figure 2. First, we exposed cells to UV-B and secondly, to RF-EMF (3.5 GHz; 0.25, 1, or 4 W/kg). Before starting processing cells for flow cytometry measurements, we carried out chemical treatments according to their different incubation times (as explained later). The "Mock" sample was handled as the "Positive Control" but without adding the chemical inductor. With the aim of investigating cooperative effect of UV-B and RF-EMF, one sample underwent both exposures, consecutively. As already explained, for each treatment, we had a specific negative control.

2.3 | Flow cytometry measurements

Flow cytometry assays were performed using a BD FACSCanto™ II instrument and the BD FACSDiva Software. Approximately 20,000 cells events were collected for each sample.

Mitochondrial stress was assessed in terms of ROS production, especially superoxide, and loss of mitochondrial membrane potential ($\Delta\Psi_m$). For this purpose, we used *MitoSOX™ Red* (Molecular Probes; Invitrogen) and *Mitostatus® TMRE* (tetramethylrhodamine ethyl ester;

1521186x, 2024, 3, Downloaded from https://onlinelibrary.wiley.com/doi/10.1002/bem.22495 by University Of British Columbia, Wiley Online Library on [10/10/2026]. See the Terms and Conditions (https://onlinelibrary.wiley.com/terms-and-conditions) on Wiley Online Library for rules of use; OA articles are governed by the applicable Creative Commons License

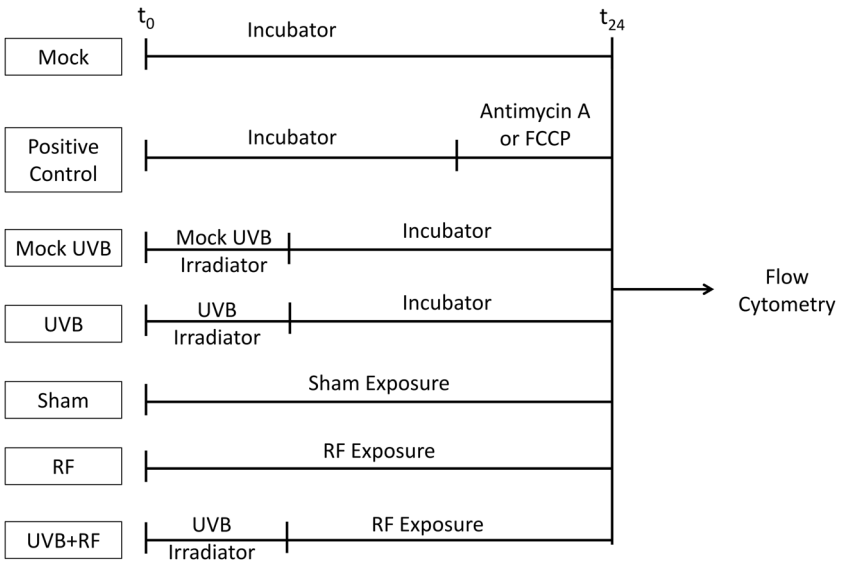


FIGURE 2 Protocol and timing of each experimental series. The day after seeding, we mock- ("Mock UVB") and UV-B exposed the cells. Immediately after, "UVB + RF" and "RF" samples underwent RF treatment (3.5 GHz; 0.25, 1, or 4 W/kg) while all controls were maintained in the incubator for 24 h. Depending on the activation times of the "positive control" (2 h for Antimycin A and 20 min for FCCP), cells underwent chemical incubation until the end of the 24 h RF exposure. On Day 3, all cells were analyzed by flow cytometry.

BD Pharmingen™) probes, respectively. Moreover, cell viability was evaluated in terms of early apoptosis and necrosis or late apoptosis induction using the *APC Annexin V* (BD Pharmingen™) and the *Sytox Blue Dead Cell Stain* (Molecular Probes; Invitrogen) fluorophores, respectively.

2.3.1 | ROS detection

To monitor the cellular metabolic state under UV-B and/or RF-EMF exposure, we used the validated *MitoSOX™ Red* probe.

Based on the literature (Kauffman et al., 2016; Mukhopadhyay et al., 2007; Wang et al., 2015), we adapted the experimental protocol to our biological system. To validate ROS generation, we used a well-known inhibitor of mitochondrial electron transport, the *Antimycin A* (Antimycin A from *Streptomyces* sp; Sigma-Aldrich), at final concentration of 205.3 µM (Xp6be cells) or 11.7 µM (KHAT cells) in the culture medium. The chemical product was added on attached cells for 2 h, at 37°C. Then, cells were washed with PBS and stained with *MitoSOX™ Red* at a final concentration of 2.5 µM, for 30 min, in the dark. The excess of probe was eliminated, and cells were detached using 500 µl of *Trypsin-EDTA* solution and collected into 5 ml cytometry tubes for two cycles of washing centrifugation (5 min, 1200 rpm, room temperature, RT) in Hanks's balanced salt solution (*Gibco™ HBSS*; Thermo Fischer Scientific).

Finally, *Sytox Blue Dead Cell Stain* (0.6 µM for Xp6be cells and 3 µM for KHAT cells) was loaded for 5 min in the dark, at RT. During flow cytometry assays, cells were kept on ice to minimize degradation.

All measurements were performed under blind conditions by coding the samples.

2.3.2 | Change in mitochondrial membrane potential ($\Delta\Psi_m$) and apoptosis detection

$\Delta\Psi_m$ and apoptosis were monitored using the *Mitostatus® TMRE* dye which is a highly fluorescent, cationic probe able to accumulate inside mitochondria of healthy cells, depending on their inner membrane potential. Nonapoptotic or cells with polarized mitochondria emit fluorescence, which intensity progressively decreases with changes in $\Delta\Psi_m$ or occurrence of early apoptosis (See Supporting Information S1: Supplementary data).

For each series of experiments, we included a positive control by using the *carbonyl cyanide p-(trifluormethoxy)phenylhydrazone* reactive (FCCP, Tocris Bio-Techne), a well-known uncoupler of oxidative phosphorylation. It was incubated with cells at the final concentration of 7.16 µM (for Xp6be cells) or 3.80 µM (for KHAT), in HBSS, for 20 min at 37°C.

Mitostatus®TMRE was directly added to adherent cells that reached at least 70% of confluence: cells were washed with PBS and loaded in HBSS with 200 nM of the fluorescent dye, for 20 min at 37°C, in the dark. Then, cells were collected into 5 ml cytometry tubes for two cycles of washing centrifugation (5 min, 1200 rpm, RT) in HBSS buffer.

Finally, samples were loaded with *Annexin V* (5 µl) and *Sytox Blue Dead Cell Stain* dyes (0.6 µM for Xp6be

15231186x, 2024, 3, Downloaded from https://onlinelibrary.wiley.com/doi/10.1002/bem.22495 by University Of British Columbia, Wiley Online Library on [10/10/2026]. See the Terms and Conditions (https://onlinelibrary.wiley.com/terms-and-conditions) on Wiley Online Library for rules of use; OA articles are governed by the applicable Creative Commons License

cells and 3 µM for KHAT cells), and processed for flow cytometry. During the assay, cells were kept on ice to minimize degradation.

All measurements were performed under blind conditions by coding the samples.

2.4 | Statistical analysis

Each independent experiment was performed six times in duplicate, pooled, and analyzed using the unpaired two-sample Wilcoxon rank sum test. $p < 0.05$ were considered statistically significant.

Dose-response curves are presented as mean ± SD of at least three experiments.

Analysis and curves were carried out using the GraphPad Prism software version 9.5 for Windows (GraphPad Software) and the R software (R, 2023). The GraphPad Outlier calculator was used for outlier detection.

3 | RESULTS

3.1 | Impact of 5G-modulated 3.5 GHz RF-EMF exposure alone and after UV-B pre-exposure on mitochondrial ROS production in Xp6be fibroblasts and KHAT keratinocytes

To assess the potential impact of 3.5 GHz RF-EMF on mitochondrial ROS production, we first performed a positive control where mitochondrial ROS and superoxide production were measured following incubation of either Xp6be fibroblasts or KHAT keratinocytes with increasing doses of *Antimycin A*, an inhibitor of the electron transport in the mitochondrial chain. As expected, the *MitoSOX Red* fluorescence probe increased statistically significantly with the dose of *Antimycin A* used and reached a plateau for the maximal dose of *Antimycin A* tested on either Xp6be (Figure 3a) or KHAT cells (Figure 3b). Based on these experiments, we calculated that *Antimycin A* displays an EC_{50} of 205.3 and 11.17 µM on Xp6be and KHAT cells, respectively, which is in line with the values found on other cell types (Wang et al., 2015).

Since our study also aimed at assessing the potential interaction between RF-EMF and UV-B exposure, we next verified that UV-B exposure triggers ROS and superoxide production in Xp6be and KHAT cells. These cells were therefore irradiated with increasing doses of UV-B up to 18 ± 0.38 mJ/cm^2, which triggered an almost twofold increase in ROS production in both cell lines but without reaching a plateau (Figure 4a,b). Of note, a higher dose of 43.93 ± 0.40 mJ/cm^2 was tested but excluded from our analysis as it was found highly cytotoxic, that is, inducing necrosis in about 30% of the cell population. Moreover, at 18 ± 0.38 mJ/cm^2, ROS level detected in human keratinocytes was statistically significantly higher than the corresponding control level (Figure 4b). According to our dose-response experiment, we exposed Xp6be and KHAT cells to 5.08 ± 0.63 mJ/cm^2 (Figure 4c) and 16.4 ± 1.03 mJ/cm^2 (Figure 4d), respectively, since these UV-B doses triggered about 50% of the maximal response detected at 18 ± 0.38 mJ/cm^2 in each cell type. This result confirms that UV-B irradiation induces ROS production (Heck et al., 2003; Paz et al., 2008).

After fine-tuning our experimental conditions, we examined the ROS production in human Xp6be fibroblasts and KHAT keratinocytes exposed to 5G-modulated 3.5 GHz RF-EMF at three SAR levels (0.25, 1, and 4 W/kg) for 24 h (Figure 5). Our results point to a statistically significant decrease (about 15%) of mitochondrial ROS level in Xp6be cells that were exposed to RF-EMF at 1 W/kg (Figure 5a). However, ROS production was not modified after RF-EMF exposure of Xp6be at either 0.25 or 4 W/kg and no difference

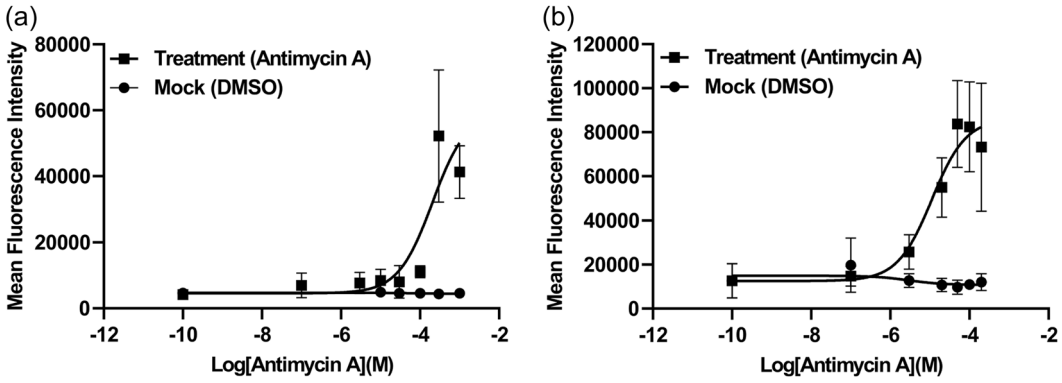


FIGURE 3 Mitochondrial reactive oxygen species (ROS) production under Antimycin A treatment. (a) Dose-response curves of Antimycin A-induced activity in Xp6be fibroblasts activated for 2 h at 37°C with increasing concentration of the compound. (b) Dose-response of Antimycin A in KHAT keratinocytes under the same incubation conditions. The level of ROS is expressed as the mean fluorescence intensity of the MitoSOX Red probe. The results represent the average ± SD of $n = 3$ experiments for each cell type.

15231186x, 2024, 3, Downloaded from https://onlinelibrary.wiley.com/doi/10.1002/bem.22495 by University Of British Columbia, Wiley Online Library on [10/10/2026]. See the Terms and Conditions (https://onlinelibrary.wiley.com/terms-and-conditions) on Wiley Online Library for rules of use; OA articles are governed by the applicable Creative Commons License

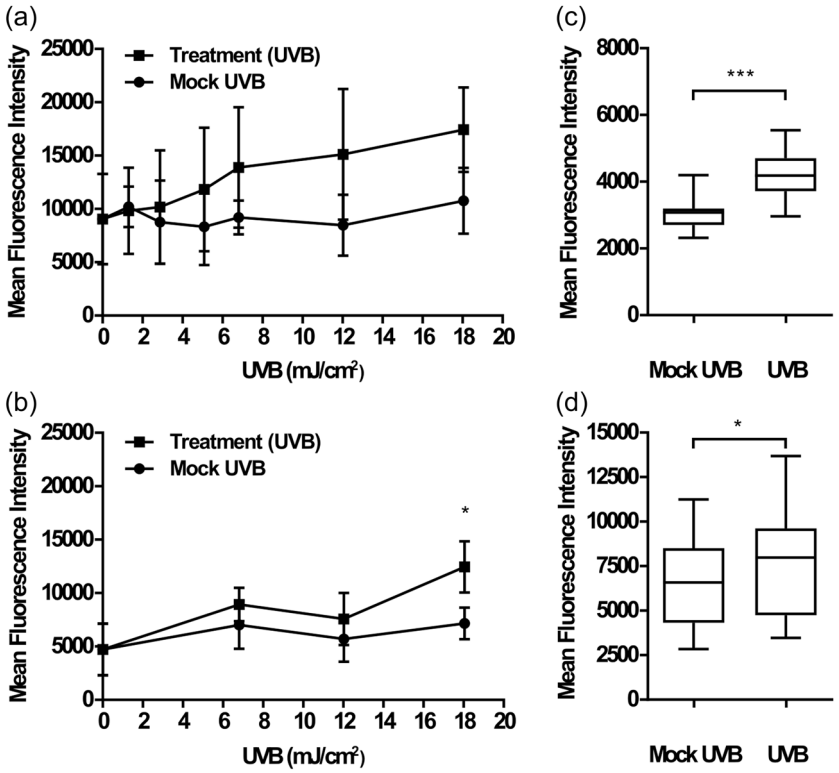


FIGURE 4 Mitochondrial reactive oxygen species (ROS) production under UV-B irradiation. (a) Xp6be fibroblasts were irradiated or mock-irradiated with increasing doses of UV-B and the concentration of ROS was measured 24 h after treatment. The results represent the average ± SD of at least $n = 3$ experiments. (b) KHAT keratinocytes were irradiated and mock-irradiated with increasing doses of UV-B. The level of ROS is expressed as the mean fluorescence intensity of the MitoSOX Red probe. The results represent the average ± SD of at least $n = 3$ experiments. (c) The whiskers box graphs show the difference of the ROS production measured in Xpd6be fibroblasts irradiated with UV-B at 5 ± 0.63 mJ/cm^2 and the mock-irradiated cells. (d) The whiskers box graphs show the difference of the ROS production measured in KHAT cells irradiated with UV-B at 16.4 ± 1.03 mJ/cm^2 and the mock-irradiated cells. Data from $n = 18$ experiences in duplicate were pooled and analyzed using the unpaired two-sample Wilcoxon rank sum test (*$p < 0.05$; ***$p < 0.001$).

could be measured between sham- and RF-EMF exposed KHAT keratinocytes, whatever the SAR (Figure 5b). We also investigated whether such exposure could enhance or reduce the effect of an intermediate dose of UV-B. Interestingly, RF-EMF exposure of keratinocytes statistically significantly enhanced the UV-B-induced ROS production by 28% and 20% at 0.25 and 1 W/kg, respectively. We observed a 16% difference between UV-B pre-irradiated cells subsequently exposed to RF-EMF at 4 W/kg and those pre-irradiated with UV-B and sham-exposed to RF-EMF. However, the difference was not statistically significant (Figure 5d).

3.2 | Impact of 5G-modulated 3.5 GHz RF-EMF exposure alone and after UV-B pre-exposure on the mitochondrial membrane potential ($\Delta\Psi_m$) in Xp6be fibroblasts and KHAT keratinocytes

We next investigated whether 5G-modulated 3.5 GHz RF-EMF signal could impact mitochondrial integrity through changes in the $\Delta\Psi_m$ of Xp6be and KHAT cells preirradiated or not with UV-B. We also evaluated cellular apoptosis or necrosis, as they are known to be correlated with changes in the $\Delta\Psi_m$ (Paz et al., 2008).

We first assessed the variations of $\Delta\Psi_m$ following incubation with carbonyl cyanide *4-(trifluoromethoxy) phenylhydrazone (FCCP)*, a mitochondrial uncoupler able to dissipate the gradient of protons across the inner membrane (O'Brien et al., 1978). As expected, we observed that FCCP dose-dependently increased the percentage of cells with dissipated $\Delta\Psi_m$, with an EC_{50} of 7.16 and 3.80 µM in Xp6be and KHAT cells, respectively (Figure 6a,b). These values are close to data from previous works (Han et al., 2010; Kondapalli et al., 2012), thereby demonstrating the high sensitivity of the assay to measure $\Delta\Psi_m$ variations in Xp6be and KHAT cells.

We next assessed whether irradiation with increasing doses of UV-B also trigger changes in $\Delta\Psi_m$ in Xp6be and KHAT cells, as documented from the literature (Denning et al., 2002; Lee et al., 2013). Both cell lines were therefore irradiated with

1521186x, 2024, 3, Downloaded from https://onlinelibrary.wiley.com/doi/10.1002/bem.22495 by University Of British Columbia, Wiley Online Library on [10/10/2026]. See the Terms and Conditions (https://onlinelibrary.wiley.com/terms-and-conditions) on Wiley Online Library for rules of use; OA articles are governed by the applicable Creative Commons License

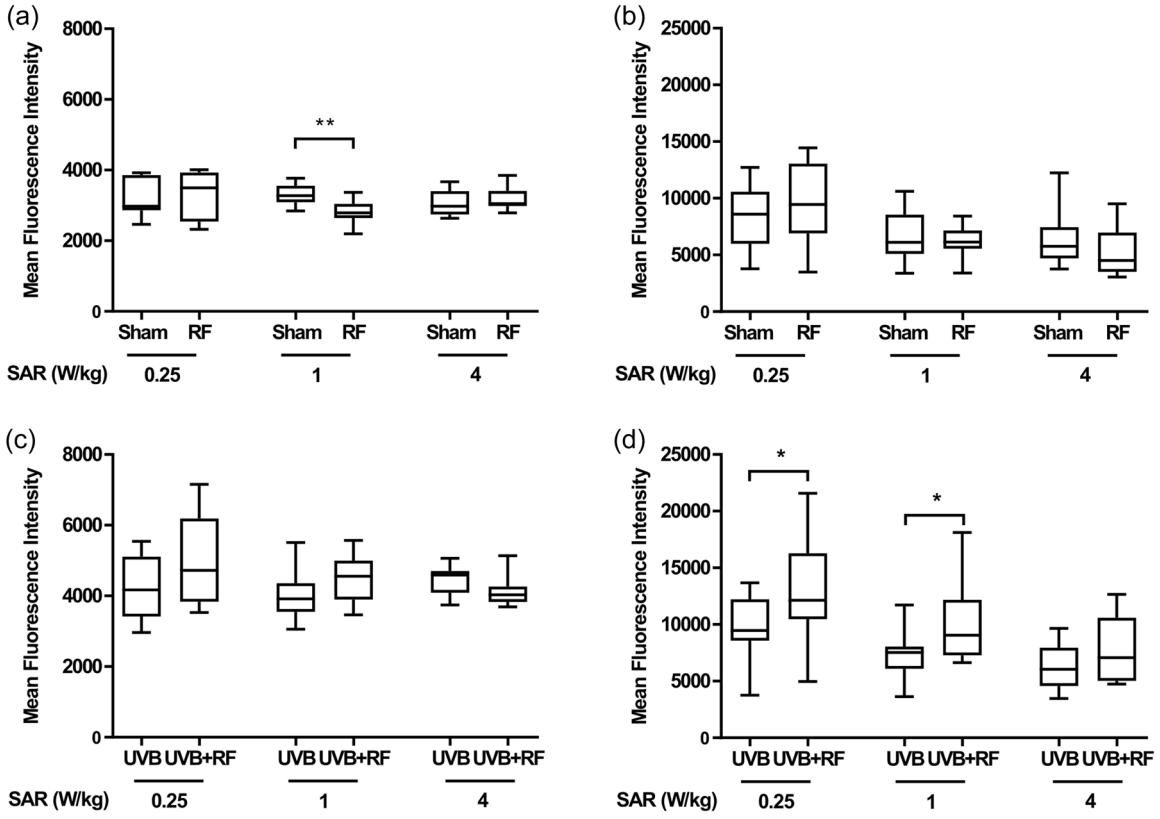


FIGURE 5 Effect of 5G-modulated 3.5 GHz signal on mitochondrial reactive oxygen species (ROS) generation. (a) Xp6be fibroblasts and (b) KHAT keratinocytes were exposed or sham-exposed to radiofrequency electromagnetic fields (RF-EMF) at different specific absorption rate (0.25, 1, 4 W/kg). (c) Xp6be fibroblasts and (d) KHAT keratinocytes were pre-irradiated with UV-B and then to RF-EMF at 0.25, 1, 4 W/kg and compared with the UV-B preirradiated and RF sham-exposed samples. Data from six independent experiments in duplicate were pooled and analyzed using the unpaired two-sample Wilcoxon rank sum test (*$p < 0.05$, **$p < 0.01$).

different doses of UV-B, and the measurement of $\Delta\Psi_m$ change was performed 24 h later. As expected, UV-B irradiation dose-dependently decreased $\Delta\Psi_m$ in both Xp6be fibroblasts (Figure 7a) and KHAT keratinocytes (Figure 7b). We measured a six-fold increase in the percentage of cells showing a decreased $\Delta\Psi_m$ when both cell types were irradiated with $101.5 \pm 1.30\ mJ/cm^2$ of UV-B, that is, the maximal dose tested. Based on this result, we estimated that the dose corresponding to 50% of the maximal effect detected was $30.6 \pm 0.12\ mJ/cm^2$ in the Xp6be fibroblasts and $43.93 \pm 0.40\ mJ/cm^2$ in KHAT

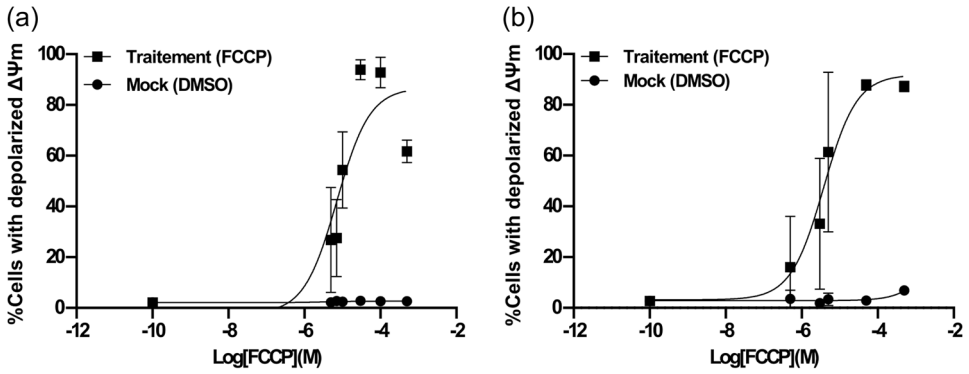


FIGURE 6 Loss in mitochondrial membrane potential ($\Delta\Psi_m$) under FCCP treatment. (a) Dose-response curves of FCCP-treated Xp6be fibroblasts and (b) dose-response curves of FCCP-treated KHAT keratinocytes. Cells were treated for 20 min at 37°C with increasing concentrations of the proton ionophore. The effect is expressed as percentage of cells exhibiting $\Delta\Psi_m$. No change occurred in the presence of the solvent (DMSO). The results represent the average ± SD of $n = 3$ experiments for each cell types.

15321866x, 2024, 3, Downloaded from https://onlinelibrary.wiley.com/doi/10.1002/bem.22495 by University Of British Columbia, Wiley Online Library on [10/10/2026]. See the Terms and Conditions (https://onlinelibrary.wiley.com/terms-and-conditions) on Wiley Online Library for rules of use; OA articles are governed by the applicable Creative Commons License

keratinocytes, the latter being in line with another report on the same cell line (Paz et al., 2008).

We confirmed, in independent experiments, that UV-B irradiation of Xp6be (Figure 7c) and KHAT cells (Figure 7d) with these doses led to a 3.5- and 2.4-fold decrease in $\Delta\Psi_m$, respectively.

Moreover, UV-B induced a fivefold and fourfold higher percentage of apoptotic and necrotic cells population, respectively, in Xp6be fibroblasts in comparison to mock-irradiated cells (Figure 8a). Similarly, KHAT keratinocytes showed a 1.68-fold statistically significant increase in apoptotic population, and a 13.3% increase in necrotic cells (Figure 8b).

These results confirm that UV-B irradiation can be properly used as a positive control for induction of apoptosis and necrosis, as documented in the literature (Denning et al., 2002; Lee et al., 2013).

We finally assessed whether exposing Xp6be fibroblasts (Figure 9) and KHAT keratinocytes (Figure 10) to the 5G-modulated 3.5 GHz signal at three different SAR values, that is, 0.25, 1, and 4 W/kg, for 24 h, impact the mitochondrial integrity and the cellular viability either directly or following UV-B irradiation. Whatever SAR and biological endpoint, we did not detect any statistically significant difference between sham-exposed and RF-EMF-exposed conditions in Xp6be and KHAT cells. Similarly, RF-EMF exposure did not statistically significantly modify the capacity of the UV-B irradiation to trigger $\Delta\Psi_m$ diffusion, early apoptosis, or necrosis in both cell types.

4 | DISCUSSION

In our daily environment, we are constantly exposed to UV-B radiations and to RF-EMF used for wireless communication (e.g., mobile phones, 5G, TV, radio). Therefore, we investigated whether continuous exposure, in isothermal conditions, to 5G-modulated 3.5 GHz RF-EMF signal at 0.25, 1, and 4 W/kg could trigger mitochondrial ROS synthesis, change in membrane potential and cellular apoptosis in Xp6be human fibroblast and KHAT keratinocyte cell lines. To assess a potential interaction between 5G RF-EMF and UV-B, human Xp6be fibroblasts and KHAT keratinocytes were pre-treated with UV-B. In experiments with UV-B, we used doses triggering 50% of

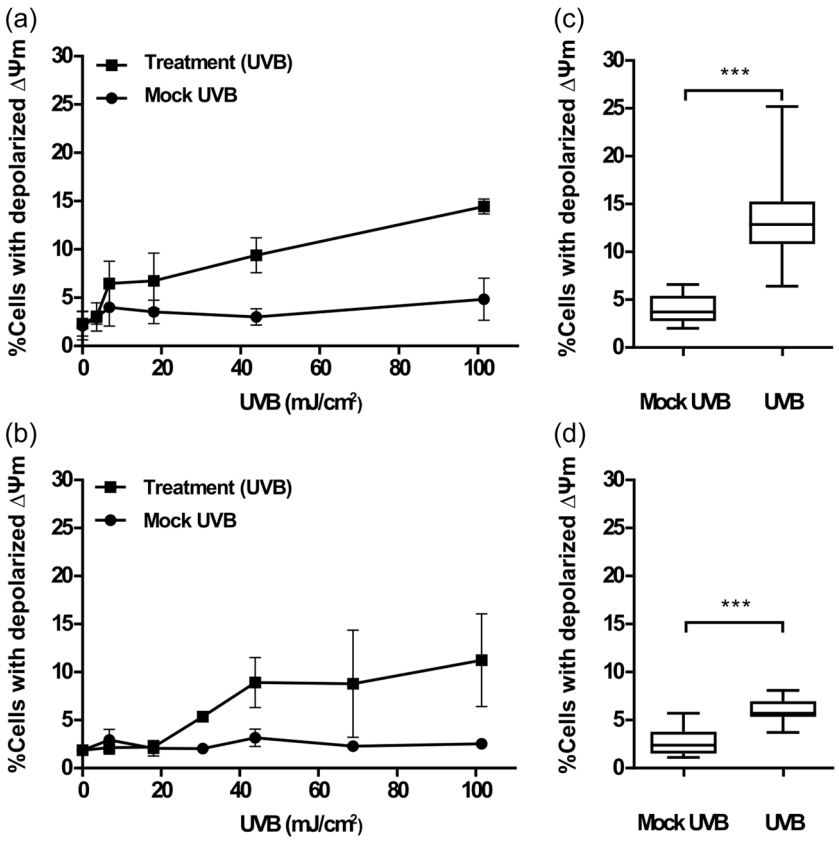


FIGURE 7 Variation of the mitochondrial membrane potential ($\Delta\Psi$m) under UV-B irradiation. Xp6be fibroblasts (a) and KHAT keratinocytes (b) were irradiated and mock-irradiated with increasing doses of UV-B and $\Delta\Psi$m was measured 24 h after treatment. The results are expressed as percentage of cells showing $\Delta\Psi$m changes. Average ± SD of at least $n = 3$ experiments are presented. The whiskers box graphs show the $\Delta\Psi$m of cells mock UV-irradiated or irradiated with UV-B dose of 30.6 ± 0.11 mJ/cm^2 in fibroblasts (c). The whiskers box graphs show the $\Delta\Psi$m of cells mock UV-irradiated or irradiated with UV-B dose of 43.93 ± 0.4 mJ/cm^2 in keratinocytes (D). Data from $n = 18$ experiences in duplicate were pooled and analyzed using the unpaired two-sample Wilcoxon rank sum test (***$p < 0.001$).

1521186x, 2024, 3, Downloaded from https://onlinelibrary.wiley.com/doi/10.1002/bem.22495 by University Of British Columbia, Wiley Online Library on [10/10/2026]. See the Terms and Conditions (https://onlinelibrary.wiley.com/terms-and-conditions) on Wiley Online Library for rules of use; OA articles are governed by the applicable Creative Commons License

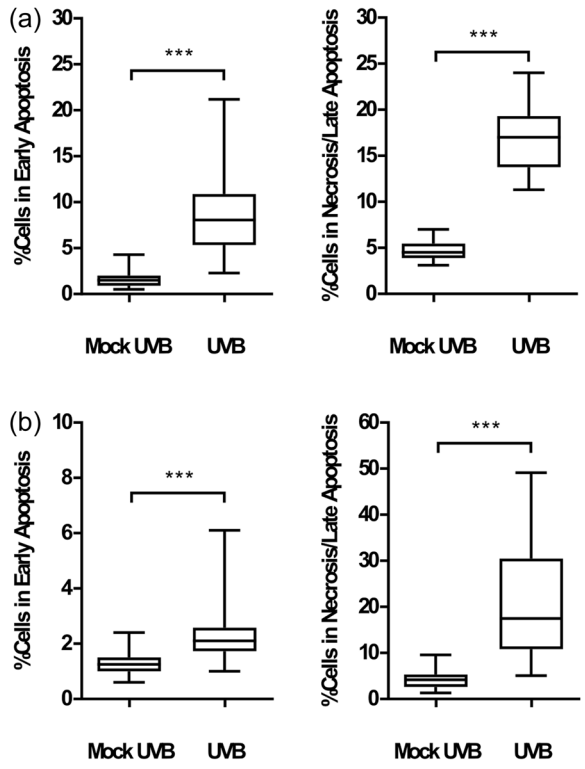


FIGURE 8 Effect of UV-B irradiation on early apoptosis (left panel) and necrosis (right panel). (a) Xp6be fibroblasts irradiated with $30.6 \pm 0.12\ mJ/cm^2$ and (b) KHAT keratinocytes irradiated with to $43.93 \pm 0.40\ mJ/cm^2$. Data from $n = 18$ experiences in duplicate were pooled and analyzed using the unpaired two-sample Wilcoxon rank sum test (***$p < 0.001$).

the maximal effect in order to measure either a synergistic or protective mechanism of the subsequent 5G RF-EMF exposure. Of interest, we always remained in the range of environmental conditions, around $30\ mJ/cm^2$, the standard erythemal dose (SED) for untanned, lightly pigmented skin (ICNIRP, 2004).

We previously showed that RF-EMF exposures at 1.8 GHz (Enhanced Data rate for GSM Evolution, EDGE modulation, 2 and 10 W/kg) did not induce ROS production in various human brain cells (SH-SY5Y, U87, and CHME5 cell lines), nor in rat primary cortical neurons (De Gannes et al., 2011). In the present work, mitochondrial ROS concentration was statistically significantly reduced in Xp6be fibroblasts that were exposed for 24 h to 5G-modulated 3.5 GHz RF-EMF at 1 W/kg, but not at 0.25 and 4 W/kg. In KHAT keratinocytes exposed to 5G RF-EMF, mitochondrial ROS concentration was not modified whatever the SAR used. Moreover, there was no impact of 5G RF-EMF exposure on mitochondrial membrane potential ($\Delta\Psi_m$) and apoptosis, in either cell types.

While a large number of papers investigated whether RF-EMF in the GHz range induce oxidative stress and ROS production (Schuermann & Mevissen, 2021; Wang & Zhang, 2017), only a few of them used fibroblasts (from skin or other tissues) and keratinocytes.

First, a decreased concentration in mitochondrial ROS level, as seen in our study using Xp6be fibroblasts exposed at 1 W/kg, is not commonly reported in the literature. To the best of our knowledge, only one study already reported a transient decreased mitochondrial ROS concentration in mature mouse spermatozoa exposed for 1 h to 1.8 GHz RF-EMF at 1.5 W/kg (Houston et al., 2018). Interestingly, the same result was not reproduced for longer exposure, lower SAR level (i.e., 0.15 W/kg) nor in other cell types. More recently, in line with the present results, Xu et al. (2013) found no modification in the intracellular ROS concentration in six cell types, among which human skin fibroblasts, exposed to GSM-modulated 1.8 GHz RF-EMF at 3 W/kg for 1 or 24 h (Xu et al., 2013). At 0.15 W/kg, Houston et al. (2018) also reported no change in mitochondrial ROS production in McCoy mouse fibroblasts that were exposed to an unmodulated 1.8 GHz signal for 2 and 6 h (Houston et al., 2018). Finally, Zeni et al. (2007) found no change in ROS production in L929 fibroblasts exposed to either continuous-wave (CW) and GSM mobile phone signals (900 MHz, 10 or 30 min) at 0.3 and 1 W/kg, which is thus partially in line with the present data (Zeni et al., 2007). By contrast, Hou et al. (2015) reported an increased ROS production in NIH/3T3 mouse embryonic fibroblasts that were intermittently exposed (5 min ON/10 min OFF) for various durations (ranging from 0.5 to 8 h) to a 1.8 GHz GSM-talk mode signal at an averaged SAR of 2 W/kg. Interestingly, this effect was maximal after 1 h and slightly and discontinuously decreased when cells were exposed for longer duration (Hou et al., 2015). Similarly, Kang et al. (2014) reported that a combination of two RF-EMF signals (837 MHz CDMA and 1950 MHz WCDMA) increased intracellular ROS production in NIH/3T3 cells when exposed for 2 h at a total SAR of 4 W/kg under isothermal conditions (Kang et al., 2014). Interestingly, the amplitude of this effect was about 30%. Finally, Cermak et al. (2017) observed that the level of superoxide radicals increased in V79 Chinese hamster lung fibroblasts exposed for 1 h to 1.8 GHz RF-EMF at 1.6 W/kg. This effect was correlated with a transient increase in the level of the antioxidant enzyme GSH observed in these cells after 10 min of RF-EMF exposure (Cermak et al., 2017).

In HaCat human keratinocytes, Kim et al. (2021) reported that a 1.76 GHz RF-EMF exposure at 4 W/kg, 2 h per day for 4 days, induced intracellular ROS production (Kim et al., 2021). The same author also shown a reduction in the ability of α-melanocyte-stimulating hormone to induce melanogenesis through decreased ROS level, in B16F10 murine melanoma cells exposed for 4 h per day up to 2 days to CW 28 GHz signal at $10\ W/m^2$ (Kim et al., 2022). Those data in the human HaCat cell line are thus contradictory and also in contrast with our findings.

Using exposures to UV-B and RF-EMF, we found that RF-EMF slightly but statistically significantly

1521186x, 2024, 3, Downloaded from https://onlinelibrary.wiley.com/doi/10.1002/bem.22495 by University Of British Columbia, Wiley Online Library on [10/10/2026]. See the Terms and Conditions (https://onlinelibrary.wiley.com/terms-and-conditions) on Wiley Online Library for rules of use; OA articles are governed by the applicable Creative Commons License

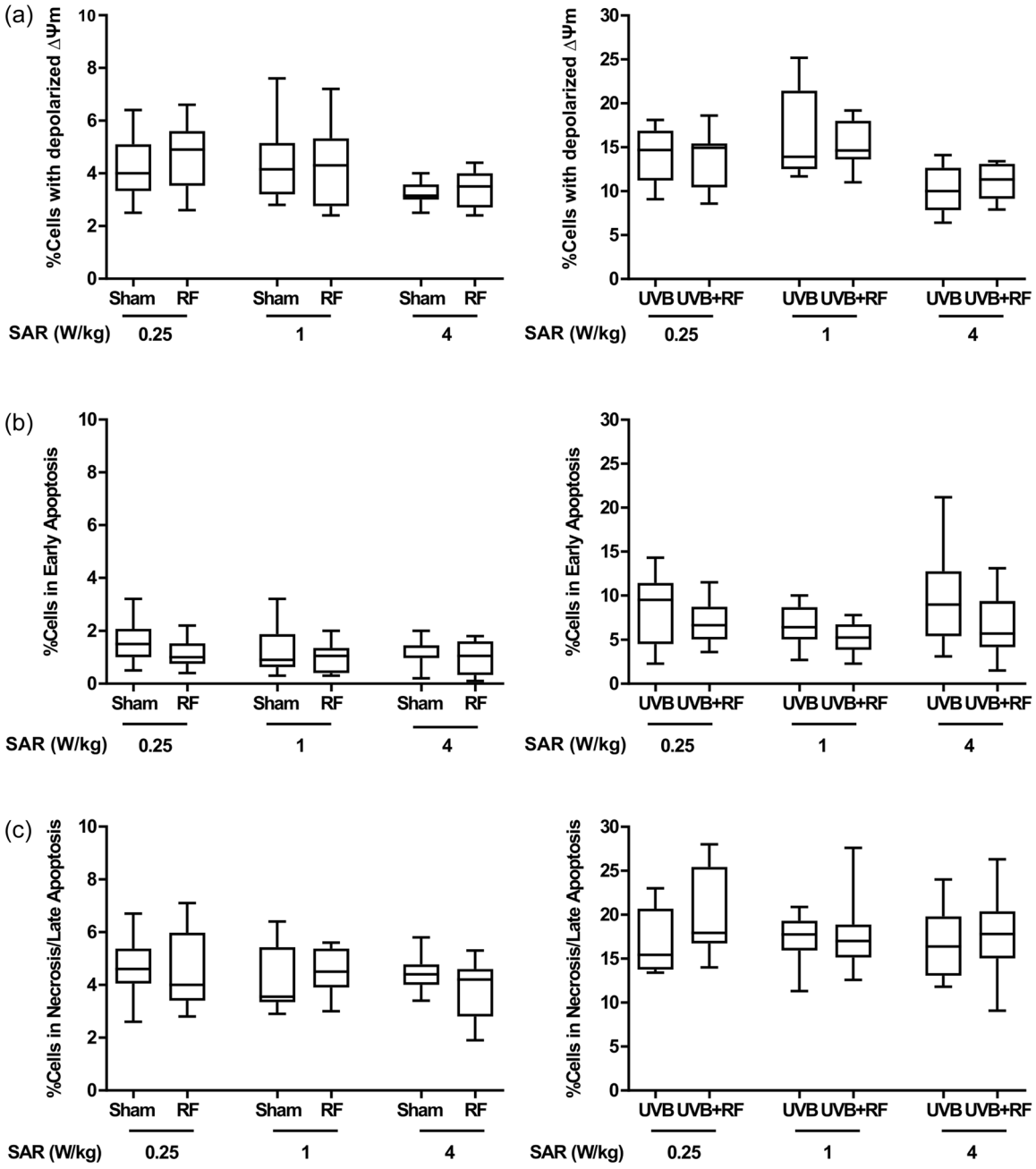


FIGURE 9 Effects of 5G-modulated 3.5 GHz exposures on (a) mitochondrial membrane potential ($\Delta\Psi$m), (b) early apoptosis, and (C) necrosis in Xp6be fibroblasts (left panel). Each RF-EMF exposed group at 0.25, 1, and 4 W/kg was compared to its corresponding sham-exposed group. In the right panel, the effect of the UV-B and RF-EMF exposure was analyzed on (a) mitochondrial membrane potential ($\Delta\Psi$m), (b) early apoptosis, and (c) necrosis at different SAR. Each UV-B + RF-EMF exposed group was compared to its corresponding UV-B irradiated group. Data from $n = 6$ experiences in duplicate were pooled and analyzed using the unpaired two-sample Wilcoxon rank sum test.

increased UV-B-induced ROS generation at 0.25 and 1 W/kg in KHAT keratinocytes, without detecting any variation in $\Delta\Psi_m$ or cellular apoptosis, whatever SAR considered. By contrast, no effect was found in Xp6Be fibroblasts exposure to UV-B, whatever the biological readout or SAR level tested.

To the best of our knowledge, only four studies have investigated the combined effect of RF-EMF and UV radiations on skin in vitro or in vivo. In a former study, Meltz et al. (1987) showed that following an initial UV irradiation (1.4 J/m^2/s for 15 s, UV type not indicated) to trigger DNA breaks, DNA repair was not affected in MRC-5 normal human diploid fibroblasts exposed from 1 h and up to 3 h to 350, 850, and 1200 MHz signals, at maximum SAR of 0.39 ± 0.15, 4.5 ± 3.0, and 2.7 ± 1.6 W/kg, respectively (Meltz et al., 1987). Fifteen years later, Heikkinen et al. (2003) assessed the potential effects of RF-EMF on

15211866, 2024, 3, Downloaded from https://onlinelibrary.wiley.com/doi/10.1002/bem.22495 by University Of British Columbia, Wiley Online Library on [10/10/2026]. See the Terms and Conditions (https://onlinelibrary.wiley.com/terms-and-conditions) on Wiley Online Library for rules of use; OA articles are governed by the applicable Creative Commons License

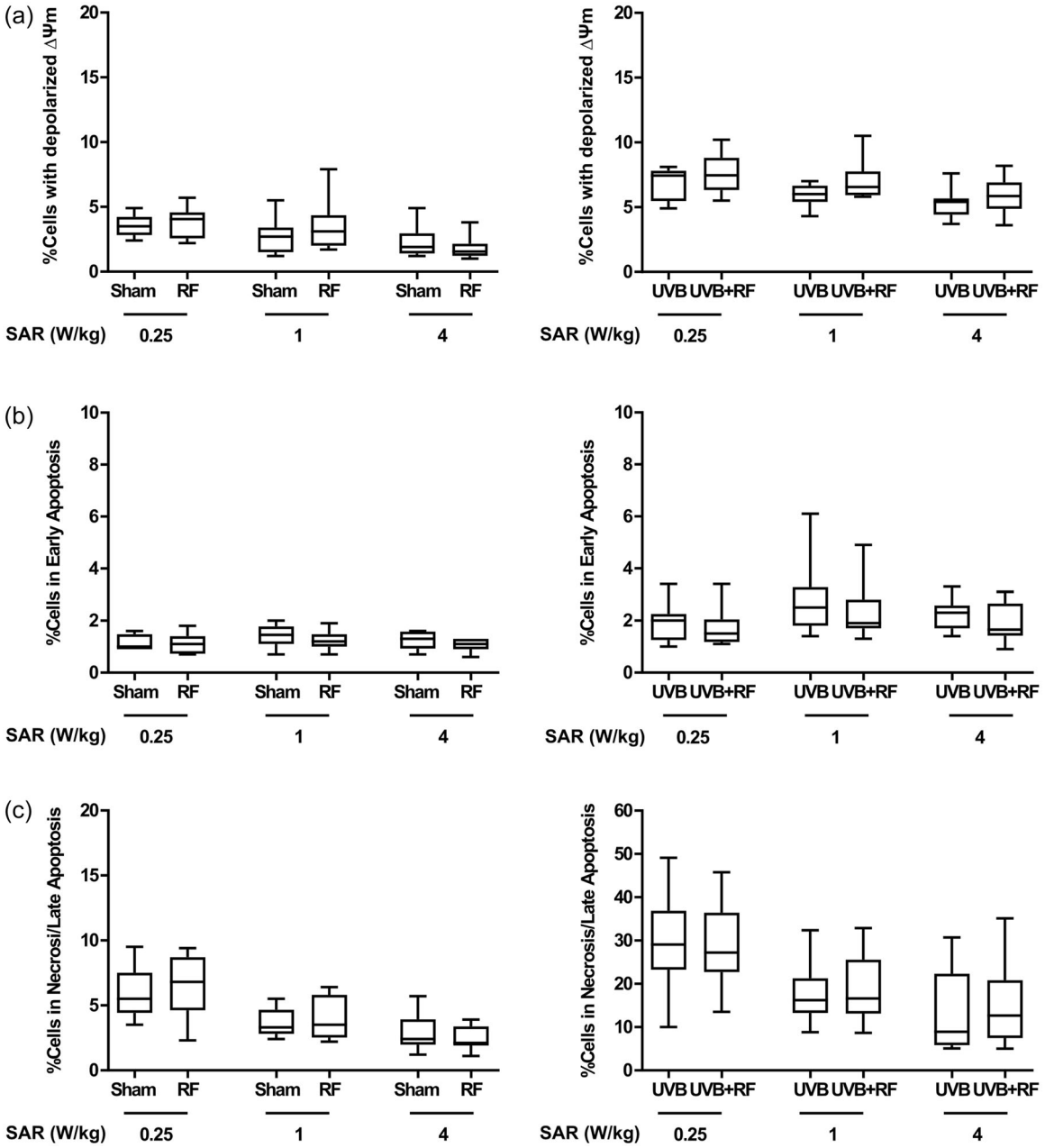


FIGURE 10 Effects of 5G-modulated 3.5 GHz exposures on (a) mitochondrial membrane potential (ΔΨm), (b) early apoptosis, and (c) necrosis in KHAT keratinocytes. Each RF-exposed group was compared to its sham-exposed group at 0.25, 1, and 4 W/kg (left panel). On the right panel, the effect of the UV-B and RF-EMF exposure was analyzed on (A) mitochondrial membrane potential (ΔΨm), (b) early apoptosis, and (c) necrosis the different SAR. Each UV-B + RF-EMF exposed group was compared to its corresponding UV-B irradiated group. Data from $n = 6$ experiences in duplicate were pooled and analyzed using the unpaired two-sample Wilcoxon rank sum test.

UV-induced skin tumorigenesis in ornithine decarboxylase (ODC) overexpressing transgenic and non-transgenic mice. ODC-overexpressing transgenic mice are predisposed to skin tumors development. Mice were exposed for 52 weeks to UV radiation or a combination of UV radiation and RF-EMF (0.5 W/kg whole-body, 1.5 h a day, 5 days a week). The animals were exposed to UV radiation using lamps simulating the solar spectrum with a dose of 24 mJ/cm² delivered three times a week. One group of animals was exposed to Digital Advanced Mobile Phone System (DAMPS)-type signal at 849 MHz. The other group was exposed to GSM-modulated signal at 902.4 MHz. RF-EMF exposure did not statistically significantly affect the number of UV-induced skin tumors detected at the end of the experiment nor UV-induced skin tumor development, whatever signal considered (Heikkinen et al., 2003).

More recently, Szilágyi et al. evaluated whether combined exposure of UV (2–4 SED, wavelenghts ≥295 nm with UVB, UVA, and visible light) and either

1521186x, 2024, 3, Downloaded from https://onlinelibrary.wiley.com/doi/10.1002/bem.22495 by University Of British Columbia, Wiley Online Library on [10/10/2026]. See the Terms and Conditions (https://onlinelibrary.wiley.com/terms-and-conditions) on Wiley Online Library for rules of use; OA articles are governed by the applicable Creative Commons License

Wi-Fi-modulated 2.422 GHz signal or Universal Mobile Telecommunications System (UMTS)-modulated 1.95 GHz signal affected inflammation-related cytokine production in a 3D-reconstructed human skin model (Szilágyi et al., 2020, 2023). In the first experimental protocol, reconstructed skin was first irradiated with a UV dose of two SED before being intermittently exposed (20 min ON/20 min OFF) to RF-EMF at 4 W/kg for 24 h to assess a potential additive effect of RF-EMF exposure on UV-induced inflammatory effects on skin. In the second experimental protocol, reconstructed skins were continuously exposed to RF-EMF at 1.5 W/kg for 24 h before being irradiated with a UV dose of four SED to assess a potential adaptive response triggered by a prior RF-EMF exposure on UV-induced skin inflammation. All biological tests were performed 24 h after the last UV irradiation or RF-EMF exposure, and a delay of 4 h was set between UV and RF-EMF exposure period whatever the protocol used (Szilágyi et al., 2020). Although some nonstatistically significant changes were seen, the authors found no evidence for a proinflammatory effect in 3D skin models exposed to either RF-EMF signal alone or in combination with UV radiations (Szilágyi et al., 2023).

Thus, the present work shows, for the first time, an interaction between UV-B radiation and RF-EMF exposure on ROS production, under specific exposure conditions in human keratinocytes. By contrast, RF-EMF exposure alone was not found to increase mitochondrial ROS production. As suggested in studies showing a pro-oxidant effect of RF-EMF, ROS production is seen as a rapid and transient response that decreases with time due to activation of the antioxidant pathways (Cermak et al., 2017; Hou et al., 2015; Schuermann & Mevissen, 2021; Xu et al., 2013). Taking that into consideration, we can hypothesize that, although a 24 h-exposure did not allow us to record a long-lasting response to RF-EMF, that is, increased ROS production, this exposure may have either induced a primary ROS production that impacted the UV-induced radical stress or impeded the activity of antioxidant enzymes in human skin keratinocytes.

Exposure to RF-EMF and other agents known as ROS inducers in other cell types also showed different outcomes. No interaction of RF-EMF (CW and GSM-modulated signal at 900 MHz at 0.3 and 1 W/kg) with 3-chloro-4-(dichloromethyl)-5-hydroxy-2(5H)-furanone could be observed in L929 murine fibroblasts in terms of ROS production (Zeni et al., 2007). While the uptake of ultrafine particles by Mono Mac 6 cells was shown to induce a statistically significant increase of extracellular superoxide radical anion production, no interaction were seen when cells where exposed to CW or modulated (GSM or GSM-non DTX) RF-EMF at 900 MHz and 2 W/kg (Simkó et al., 2006). Using different cell types, Kang et al. (2014) found that the combination of two RF-EMF signals (CDMA plus WCDMA signals, 4 W/kg, 2 h) did not interact with the ROS production induced either by H_2O_2 or menadione treatments (Kang et al., 2014). By contrast, induction of ROS production was found in SH-SY5Y neuroblastoma cells exposed to a CW 872 MHz signal at 5 W/kg following a pretreatment with menadione (Luukkonen et al., 2009).

In summary, based on the available literature, including the present piece of work, papers that assessed the impact of RF-EMF on skin models in vitro or in vivo are still few and heterogeneous in terms of experimental conditions such as cell type, RF-EMF frequency, absence or presence of a RF-EMF signal modulation, and exposure duration, as well as the biological outcomes in terms of ROS production. This prevents any unequivocal conclusion on their impact on free radical production and oxidative stress.

In the present work, we found evidence that keratinocytes are more responsive to RF-EMF than skin fibroblasts after UV-B irradiation, while skin fibroblasts, but not keratinocytes barely responded to RF-EMF exposure alone. In agreement with our findings, other authors have highlighted the cell type-dependent response to a given RF-EMF signal and under identical experimental conditions. Houston et al. (2018) for instance observed that mouse male germ cells but not mouse mature spermatogonia, McCoy mouse fibroblasts, HEK293 human epithelial kidney cells, and COV434 human granulosa cells, mitochondrial ROS production was affected by RF-EMF exposure (Houston et al., 2018). Xu et al. (2013) showed that Chinese hamster lung epithelial cells and human skin fibroblasts responded to RF-EMF exposure in terms of DNA damage, by contrast to primary rat astrocytes, human amniotic epithelial cells, human lens epithelial cells, and human umbilical vein endothelial cells (Xu et al., 2013). Kang et al. (2014) also mentioned that a combination of two 2 G signals (2 h, 4 W/kg) were increased the H_2O_2 production in three out of four cell types, that is, the SH-5YSY neuroblastoma cells were not responsive to such exposure, by contrast to NIH/3T3 mice embryo fibroblasts, U87 human glioma cells, and PC12 rat pheochromocytoma cells (Kang et al., 2014). In addition, in a recent review by Wang and Zhang (2017), conflicting trends were also reported regarding the effects of RF-EMF on ROS production, even within a single cell type (i.e., neurons) (Wang & Zhang, 2017). Moreover, no specific cell type or group of cells were reliably identified as being consistently sensitive to RF-EMF exposure.

Finally, our results did not reflect a classical dose-dependent trend in either cell type. The level of mitochondrial ROS production in Xp6be fibroblasts dropped at 1 W/kg but not at 0.25 and 4 W/kg. The level of UVB-induced ROS production increased at 0.25 and 1 W/kg, but not at 4 W/kg.

1521186x, 2024, 3, Downloaded from https://onlinelibrary.wiley.com/doi/10.1002/bem.22495 by University Of British Columbia, Wiley Online Library on [10/10/2026]. See the Terms and Conditions (https://onlinelibrary.wiley.com/terms-and-conditions) on Wiley Online Library for rules of use; OA articles are governed by the applicable Creative Commons License

Nonlinear effects have already been reported after exposure to EMF, as to the so-called "window" effect. This effect refers to the occurrence of a cellular response only using specific amplitude or frequency values, and not for the adjacent intervals. Unfortunately, the mechanisms behind this "window" effect are still not well understood and were mostly reported with extremely-low-frequency EMF (Bawin & Adey, 1976; Belyaev, 2001; Markov, 2005). Exploring these nonlinear cellular responses, we can also consider the well-known toxicological concept of hormesis that consists of a biphasic dose-response phenomenon characterized by an increased performance in response to low-doses stimulation (Agathokleous & Calabrese, 2022; Calabrese, 2008). The response of skin fibroblasts to the 5G signal in the present paper might be considered as a hormesis behavior as the response is basically U-shapped in relation with the SAR level. In a recent study, Pooam et al. (2022) evoked the hormesis response to explain the nonlinear accumulation of ROS in HEK293 cells exposed for 15 min to a 1.8 GHz RF-EMF with an incident power range between −76 and −8.5 dBm (less than 10^{-9} W of emitted power, no SAR) (Pooam et al., 2022).

A biphasic answer can also refer to the so-called "adaptive response" to RF-EMF as reported in recent years. In these papers, cells exposed to RF-EMF, used as an "adaptive dose," experience less DNA damage when exposed to a "challenging dose" of genotoxic agents than non-RF-EMF pre-exposed cells (Falone et al., 2018; Vijayalaxmi et al., 2014). However, according to these authors, the RF-EMF adaptive response needs a specific protocol to occur in cells, that is, 20-h exposure to RF-EMF followed by a 3-h resting and a 1-h treatment with a genotoxic agent such as the menadione chemical (Falone et al., 2018; Sannino et al., 2022). Such a protocol was not used in the present work.

5 | CONCLUSIONS

We report here some effects of 5G-modulated RF-EMF at 3.5 GHz on human skin cells, either alone in human fibroblasts, or after exposure to UV-B radiations in human keratinocytes. The effects were found nonlinear in relation to the SAR level and their amplitude did not exceed 30% compared to sham (fibroblasts) or to UV-B radiation (keratinocytes). Interestingly, we found no correlation with any change in the UV-B-induced mitochondrial membrane potential or apoptosis, suggesting that the RF-EMF increase in UV-B-induced ROS production was not enough to additionally impact neither mitochondrial membrane potential, apoptosis nor necrosis. To further determine whether these effects could lead to any protective effect or increase UV-B harmful bioeffects, it would be interesting to evaluate the activation of the cell's antioxidant response, that is, superoxide dismutase, glutathione, or glutathione peroxidase expression level or activity. It will also be of importance to assess whether the presence of ROS can induce end-products, such as 4-hydroxy-2-nonenal that is produced by lipid peroxidation in cells, either in skin's organoids (Sun et al., 2021) or in skin in vivo, as we previously assessed in the sera of rats exposed to a CW 2.45 GHz signal (7 h/day for 30 days, 0.16 W/kg whole-body SAR) (De Gannes et al., 2009). These approaches would indeed be more representative of the skin complexity and take into account the interaction among the different skin cells.

AUTHOR CONTRIBUTIONS

Conceptualization: Yann Percherancier, Florence Poulletier de Gannes, and Isabelle Lagroye. *Methodology*: Philippe Lévêque, Delia Arnaud-Cormos, Walid Mahfouf, and Hamid Reza Revzani. *Software*: Philippe Lévêque and Delia Arnaud-Cormos. *Validation*: Yann Percherancier, Isabelle Lagroye, Philippe Lévêque, Florence Poulletier de Gannes, and Delia Arnaud-Cormos. *Formal analysis*: Lorenza Patrignoni and André Garenne. *Investigation*: Lorenza Patrignoni, Annabelle Hurtier, Alexandre Joushomme, and Rosa Orlacchio. *Data curation*: Lorenza Patrignoni. *Writing—original draft preparation*: Lorenza Patrignoni. *Writing—review and editing*: Yann Percherancier, Florence Poulletier de Gannes, and Isabelle Lagroye. *Visualization*: Yann Percherancier, Florence Poulletier de Gannes, André Garenne, and Isabelle Lagroye. *Supervision*: Annabelle Hurtier, Yann Percherancier. *Funding acquisition*: Yann Percherancier, Florence Poulletier de Gannes, and Isabelle Lagroye. All authors have read and agreed to the published version of the manuscript.

ACKNOWLEDGMENTS

We express our special thanks to Dr Muriel Cario-Andre for kindly providing us the Xp6be fibroblasts. This research was funded by the French Agency for Food, Environmental and Occupational Health and Safety (ANSES), grant number 2019/2 RF/018, and New Aquitaine regional council under grant agreement AAPR2020A-2019-8140010 (The PHYSTRIG project).

CONFLICT OF INTEREST STATEMENT

The authors declare no conflict of interest.

DATA AVAILABILITY STATEMENT

Row data that support the findings of this study are available from the corresponding author, upon reasonable request.

ETHICS STATEMENT

In our study, the biopsies utilized in our research were pre-existing surgical specimens, which were collected

1521186x, 2024, 3, Downloaded from https://onlinelibrary.wiley.com/doi/10.1002/bem.22495 by University Of British Columbia, Wiley Online Library on [10/10/2026]. See the Terms and Conditions (https://onlinelibrary.wiley.com/terms-and-conditions) on Wiley Online Library for rules of use; OA articles are governed by the applicable Creative Commons License

at the end of the routine medical procedures for therapeutic purposes, and the inclusion of these specimens in our study posed no additional risk or burden to the patients. These pre-existing surgical specimens were fully anonymized to ensure the privacy and confidentiality of the human subjects. Hence, all patients whose surgical excision biopsies were utilized to prepare primary keratinocytes had previously signed a non-objection agreement, through which they granted explicit permission for the use of their surgical excision biopsies for research purposes, in accordance with the principles outlined in the Declaration of Helsinki.

ORCID

Lorenza Patrignoni http://orcid.org/0000-0002-6934-6136

REFERENCES

Agathokleous, E., Calabrese, E.J.: Hormesis: a general biological principle. Chem. Res. Toxicol. 35, 547–549 (2022). https://doi.org/10.1021/acs.chemrestox.2c00032

Bawin, S.M., Adey, W.R.: Sensitivity of calcium binding in cerebral tissue to weak environmental electric fields oscillating at low frequency. Proc. Natl. Acad. Sci. 73, 1999–2003 (1976). https://doi.org/10.1073/pnas.73.6.1999

Bektas, H., Algul, S., Altindag, F., Yegin, K., Akdag, M.Z., Dasdag, S.: Effects of 3.5 GHz radiofrequency radiation on Ghrelin, Nesfatin-1, and Irisin level in diabetic and healthy brains. J. Chem. Neuroanat. 126, 102168 (2022). https://doi.org/10.1016/j.jchemneu.2022.102168

Belyaev, I.: Frequency-dependent effects of ELF magnetic field on chromatin conformation in *Escherichia coli* cells and human lymphocytes. Biochim. Biophys. Acta (BBA) 1526, 269–276 (2001). https://doi.org/10.1016/S0304-4165(01)00138-6

Brieger, K., Schiavone, S., Miller, J., Krause, K.: Reactive oxygen species: from health to disease. Swiss Med. Wkly 142, w13659 (2012). https://doi.org/10.4414/smw.2012.13659

Calabrese, E.J.: Hormesis: why it is important to toxicology and toxicologists. Environ. Toxicol. Chem. 27, 1451–1474 (2008). https://doi.org/10.1897/07-541.1

Capstick, M.H., Kuehn, S., Berdinas-Torres, V., Gong, Y., Wilson, P.F., Ladbury, J.M., Koepke, G., McCormick, D.L., Gauger, J., Melnick, R.L., Kuster, N.: A radio frequency radiation exposure system for rodents based on reverberation chambers. IEEE Trans. Electromagn. Compat. 59, 1041–1052 (2017). https://doi.org/10.1109/TEMC.2017.2649885

Cermak, A.M.M., Pavicic, I., Lovakovic, B.T., Pizent, A., Trosic, I.: In vitro non-thermal oxidative stress response after 1800 MHz radiofrequency radiation. Gen. Physiol. Biophys. 36, 407–414 (2017). https://doi.org/10.4149/gpb_2017007

Christ, A., Klingenbock, A., Samaras, T., Goiceanu, C., Kuster, N.: The dependence of electromagnetic far-field absorption on body tissue composition in the frequency range from 300 MHz to 6 GHz. IEEE. Trans. Microw. Theory. Tech. 54, 2188–2195 (2006). https://doi.org/10.1109/TMTT.2006.872789

Dasgupta, S., Leong, C., Simonich, M.T., Truong, L., Liu, H., Tanguay, R.L.: Transcriptomic and long-term behavioral deficits associated with developmental 3.5 GHz radiofrequency radiation exposures in Zebrafish. Environ. Sci. Technol. Lett. 9, 327–332 (2022). https://doi.org/10.1021/acs.estlett.2c00037

Dasgupta, S., Wang, G., Simonich, M.T., Zhang, T., Truong, L., Liu, H., Tanguay, R.L.: Impacts of high dose 3.5 GHz cellphone radiofrequency on Zebrafish embryonic development. PLoS. ONE. 15, e0235869 (2020). https://doi.org/10.1371/journal.pone.0235869

Denning, M.F., Wang, Y., Tibudan, S., Alkan, S., Nickoloff, B.J., Qin, J.-Z.: Caspase activation and disruption of mitochondrial membrane potential during UV radiation-induced apoptosis of human keratinocytes requires activation of protein kinase C. Cell Death Differ. 9, 40–52 (2002). https://doi.org/10.1038/sj.cdd.4400929

EMF-Portal | Radio Frequency (10 MHz–300 GHz). https://www.emf-portal.org/en/cms/page/home/effects/radio-frequency (accessed on 24 August 2022).

Falone, S., Sannino, A., Romeo, S., Zeni, O., Santini, S., Rispoli, R., Amicarelli, F., Scarfì, M.R.: Protective effect of 1950 MHz electromagnetic field in human neuroblastoma cells challenged with menadione. Sci. Rep. 8, 13234 (2018). https://doi.org/10.1038/s41598-018-31636-7

Feldman, Y., Puzenko, A., Ben Ishai, P., Caduff, A., Davidovich, I., Sakran, F., Agranat, A.J.: The electromagnetic response of human skin in the millimetre and submillimetre wave range. Phys. Med. Biol. 54, 3341–3363 (2009). https://doi.org/10.1088/0031-9155/54/11/005

De Gannes, F.P., Haro, E., Hurtier, A., Taxile, M., Ruffié, G., Billaudel, B., Veyret, B., Lagroye, I.: Effect of exposure to the edge signal on oxidative stress in brain cell models. Radiat. Res. 175, 225–230 (2011). https://doi.org/10.1667/RR2320.1

De Gannes, F.P., Taxile, M., Duleu, S., Hurtier, A., Haro, E., Geffard, M., Ruffié, G., Billaudel, B., Lévêque, P., Dufour, P., Lagroye, I., Veyret, B.: A confirmation study of Russian and Ukrainian data on effects of 2450 MHz microwave exposure on immunological processes and teratology in rats. Radiat. Res. 172, 617 (2009). https://doi.org/10.1667/RR1541.1

Han, Y.H., Yang, Y.M., Park, W.H.: Carbonyl cyanide P-(trifluoromethoxy) phenylhydroazone induces caspase-independent apoptosis in As4.1 juxtaglomerular cells. Anticancer Res. 30, 2863–2868 (2010).

Heck, D.E., Vetrano, A.M., Mariano, T.M., Laskin, J.D.: UVB light stimulates production of reactive oxygen species. J. Biol. Chem. 278, 22432–22436 (2003). https://doi.org/10.1074/jbc.C300048200

Heikkinen, P., Kosma, V.-M., Alhonen, L., Huuskonen, H., Komulainen, H., Kumlin, T., Laitinen, J.T., Lang, S., Puranen, L., Juutilainen, J.: Effects of mobile phone radiation on UV-induced skin tumourigenesis in ornithine decarboxylase transgenic and non-transgenic mice. Int. J. Radiat. Biol. 79, 221–233 (2003). https://doi.org/10.1080/0955300031000096298

Hill, D.A., Electromagnetic theory of reverberation chambers. National Bureau of Standards, Gaithersburg, MD (1998)

Hill, D.A.: Boundary fields in reverberation chambers. IEEE Trans. Electromagn. Compat. 47, 281–290 (2005). https://doi.org/10.1109/TEMC.2005.847370

Hou, Q., Wang, M., Wu, S., Ma, X., An, G., Liu, H., Xie, F.: Oxidative changes and apoptosis induced by 1800-MHz electromagnetic radiation in NIH/3T3 cells. Electromagn. Biol. Med. 34, 85–92 (2015). https://doi.org/10.3109/15368378.2014.900507

Houston, B.J., Nixon, B., King, B.V., Aitken, R.J., De Iuliis, G.N.: Probing the origins of 1,800 MHz radiofrequency electromagnetic radiation-induced damage in mouse immortalized germ cells and spermatozoa in vitro. Front. Public Health 6, 270 (2018). https://doi.org/10.3389/fpubh.2018.00270

ICNIRP Guidelines on limits of exposure to ultraviolet radiation of wavelengths between 180 Nm and 400 Nm (incoherent optical radiation). Health Phys. 87, 171–186 (2004) https://doi.org/10.1097/00004032-200408000-00006.

ICNIRP.: Guidelines for limiting exposure to electromagnetic fields (100 kHz to 300 GHz). Health Phys. 118, 483–524 (2020). https://doi.org/10.1097/HP.0000000000001210

International Agency for Research on Cancer. A review of human carcinogens. Centre international de recherche sur le cancer, IARC monographs on the evaluation of carcinogenic risks to humans. Lyon (2012)

International Commission on Non-Ionizing Radiation Protection: ICNIRP guidelines for limiting exposure to time-varying electric,

1521186x, 2024, 3, Downloaded from https://onlinelibrary.wiley.com/doi/10.1002/bem.22495 by University Of British Columbia, Wiley Online Library on [10/10/2026]. See the Terms and Conditions (https://onlinelibrary.wiley.com/terms-and-conditions) on Wiley Online Library for rules of use; OA articles are governed by the applicable Creative Commons License

magnetic, and electromagnetic fields (up to 300 GHz). Health Phys. 74, 494–522 (1998)
Ikehata, H., Ono, T.: The mechanisms of UV mutagenesis. J. Radiat. Res. 52, 115–125 (2011). https://doi.org/10.1269/jrr.10175
Ito, H., Bassett, C.A.: Effect of weak, pulsing electromagnetic fields on neural regeneration in the rat. Clin. Orthop. Relat. Res. 181, 283–290 (1983)
Kang, K.A., Lee, H.C., Lee, J.-J., Hong, M.-N., Park, M.-J., Lee, Y.-S., Choi, H.-D., Kim, N., Ko, Y.-G., Lee, J.-S.: Effects of combined radiofrequency radiation exposure on levels of reactive oxygen species in neuronal cells. J. Radiat. Res. 55, 265–276 (2014). https://doi.org/10.1093/jrr/rrt116
Kauffman, M., Kauffman, M., Traore, K., Zhu, H., Trush, M., Jia, Z., Li, Y.: MitoSOX-based flow cytometry for detecting mitochondrial ROS. Reactive Oxygen Species 2, 361–370 (2016). https://doi.org/10.20455/ros.2016.865
Kim, J.H., Kang, D.-J., Bae, J.-S., Lee, J.H., Jeon, S., Choi, H.-D., Kim, N., Kim, H.-G., Kim, H.R.: Activation of matrix metalloproteinases and FoxO3a in HaCaT keratinocytes by radiofrequency electromagnetic field exposure. Sci. Rep. 11, 7680 (2021). https://doi.org/10.1038/s41598-021-87263-2
Kim, K., Lee, Y.S., Kim, N., Choi, H.-D., Lim, K.-M.: 5G electromagnetic radiation attenuates skin melanogenesis in vitro by suppressing ROS generation. Antioxidants 11, 1449 (2022). https://doi.org/10.3390/antiox11081449
Kolarsick, P.A.J., Kolarsick, M.A., Goodwin, C.: Anatomy and physiology of the skin. J. Dermatol. Nurses' Assoc. 3, 203–213 (2011). https://doi.org/10.1097/JDN.0b013e3182274a98
Kondapalli, C., Kazlauskaite, A., Zhang, N., Woodroof, H.I., Campbell, D.G., Gourlay, R., Burchell, L., Walden, H., Macartney, T.J., Deak, M., Knebel, A., Alessi, D.R., Muqit, M.M.K.: PINK1 is activated by mitochondrial membrane potential depolarization and stimulates Parkin E3 ligase activity by phosphorylating serine 65. Open Biol. 2, 120080 (2012). https://doi.org/10.1098/rsob.120080
Kraemer, K.H.: Sunlight and skin cancer: another link revealed. Proc. Natl. Acad. Sci. 94, 11–14 (1997). https://doi.org/10.1073/pnas.94.1.11
Krutmann, J.: The role of UVA rays in skin aging. Eur. J. Dermatol. 11, 170–171 (2001)
Lawton, S.: Skin 1: the structure and functions of the skin. Nurs. Times. 111, 30–33 (2019)
Lee, C.-H., Wu, S.-B., Hong, C.-H., Yu, H.-S., Wei, Y.-H.: Molecular mechanisms of UV-induced apoptosis and its effects on skin residential cells: the implication in UV-based phototherapy. Int. J. Mol. Sci. 14, 6414–6435 (2013). https://doi.org/10.3390/ijms14036414
Leveque, P., Reineix, A., Jecko, B.: Modelling of dielectric losses in microstrip patch antennas: application of FDTD method. Electron. Lett. 28, 539–541 (1992)
Luukkonen, J., Hakulinen, P., Mäki-Paakkanen, J., Juutilainen, J., Naarala, J.: Enhancement of chemically induced reactive oxygen species production and DNA damage in human SH-SY5Y neuroblastoma cells by 872MHz radiofrequency radiation. Mutat. Res. 662, 54–58 (2009). https://doi.org/10.1016/j.mrfmmm.2008.12.005
Markov, M.S.: "Biological Windows": a tribute to W. Ross Adey. Environmentalist 25, 67–74 (2005). https://doi.org/10.1007/s10669-005-4268-8
Meltz, M.L., Walker, K.A., Erwin, D.N.: Radiofrequency (microwave) radiation exposure of mammalian cells during UV-induced DNA repair synthesis. Radiat. Res. 110, 255 (1987). https://doi.org/10.2307/3576903
Moisan, F., Laroche-Clary, A., Auzanneau, C., Ricard, N., Pourquier, P., Robert, J., Le Morvan, V.: Deciphering the role of the ERCC2 gene polymorphism on anticancer drug sensitivity. Carcinogenesis 33, 962–968 (2012). https://doi.org/10.1093/carcin/bgs107
Mukhopadhyay, P., Rajesh, M., Haskó, G., Hawkins, B.J., Madesh, M., Pacher, P.: Simultaneous detection of apoptosis and mitochondrial superoxide production in live cells by flow cytometry and confocal microscopy. Nat. Protoc. 2, 2295–2301 (2007). https://doi.org/10.1038/nprot.2007.327
Nefzi, A: Analysis and dosimetry of the coupling of electromagnetic waves with biological tissues: application to applicator design for biomedical and study of health effects. PhD Thesis (2021)
O'Brien, T.A., Nieva-Gomez, D., Gennis, R.B.: Complex formation between the uncoupler carbonyl cyanide P-trifluoromethoxyphenylhydrazone (FCCP) and valinomycin in the presence of potassium. J. Biol. Chem. 253, 1749–1751 (1978)
Orlacchio, R., Andrieu, G., Joushomme, A., Patrignoni, L., Hurtier, A., De Gannes, F.P., Lagroye, I., Percherancier, Y., Arnaud-Cormos, D., Leveque, P.: A novel reverberation chamber for in vitro bioelectromagnetic experiments at 3.5 GHz. IEEE Trans. Electromagn. Compat. 65, 39–50 (2023). https://doi.org/10.1109/TEMC.2022.3216045
Paz, M.L., González Maglio, D.H., Weill, F.S., Bustamante, J., Leoni, J.: Mitochondrial dysfunction and cellular stress progression after ultraviolet B irradiation in human keratinocytes. Photodermatol. Photoimmunol. Photomed. 24, 115–122 (2008). https://doi.org/10.1111/j.1600-0781.2008.00348.x
Pooam, M., Jourdan, N., Aguida, B., Dahon, C., Baouz, S., Terry, C., Raad, H., Ahmad, M.: Exposure to 1.8 GHz radiofrequency field modulates ROS in human HEK293 cells as a function of signal amplitude. Commun. Integr. Biol. 15, 54–66 (2022). https://doi.org/10.1080/19420889.2022.2027698
R: The R project for statistical computing. R Foundation, Vienna, Austria. https://www.r-project.org/ (accessed on 10 March 2023). R Foundation, Vienna, Austria.
Sander, C.S., Chang, H., Hamm, F., Elsner, P., Thiele, J.J.: Role of oxidative stress and the antioxidant network in cutaneous carcinogenesis. Int. J. Dermatol. 43, 326–335 (2004). https://doi.org/10.1111/j.1365-4632.2004.02222.x
Sannino, A., Scarfì, M.R., Dufossée, M., Romeo, S., Poeta, L., Prouzet-Mauléon, V., Priault, M., Zeni, O.: Inhibition of autophagy negates radiofrequency-induced adaptive response in SH-SY5Y neuroblastoma cells. Int. J. Mol. Sci. 23, 8414 (2022). https://doi.org/10.3390/ijms23158414
Schuermann, D., Mevissen, M.: Manmade electromagnetic fields and oxidative stress—biological effects and consequences for health. Int. J. Mol. Sci. 22(7), 3772 (2021)
Serra, R., Marvin, A.C., Moglie, F., Primiani, V.M., Cozza, A., Arnaut, L.R., Huang, Y., Hatfield, M.O., Klingler, M., Leferink, F.: Reverberation chambers a La Carte: an overview of the different mode-stirring techniques. IEEE Electromagn. Compat. Mag. 6, 63–78 (2017). https://doi.org/10.1109/MEMC.2017.7931986
Sies, H., Berndt, C., Jones, D.P.: Oxidative stress. Annu. Rev. Biochem. 86, 715–748 (2017). https://doi.org/10.1146/annurev-biochem-061516-045037
Simkó, M., Hartwig, C., Lantow, M., Lupke, M., Mattsson, M.-O., Rahman, Q., Rollwitz, J.: Hsp70 expression and free radical release after exposure to non-thermal radio-frequency electromagnetic fields and ultrafine particles in human mono Mac 6 cells. Toxicol. Lett. 161, 73–82 (2006). https://doi.org/10.1016/j.toxlet.2005.08.005
Sun, H., Zhang, Y.-X., Li, Y.-M.: Generation of skin organoids: potential opportunities and challenges. Front. Cell. Dev. Biol. 9, 709824 (2021)
Szilágyi, Z., Németh, Z., Bakos, J., Kubinyi, G., Necz, P.P., Szabó, E., Thuróczy, G., Pinto, R., Selmaoui, B.: Assessment of inflammation in 3D reconstructed human skin exposed to combined exposure to ultraviolet and Wi-Fi radiation. Int. J. Mol. Sci. 24, 2853 (2023). https://doi.org/10.3390/ijms24032853
Szilágyi, Z., Németh, Z., Bakos, J., Necz, P.P., Sáfár, A., Kubinyi, G., Selmaoui, B., Thuróczy, G.: Evaluation of inflammation by

1521186x, 2024, 3, Downloaded from https://onlinelibrary.wiley.com/doi/10.1002/bem.22495 by University Of British Columbia, Wiley Online Library on [10/10/2026]. See the Terms and Conditions (https://onlinelibrary.wiley.com/terms-and-conditions) on Wiley Online Library for rules of use; OA articles are governed by the applicable Creative Commons License

cytokine production following combined exposure to ultraviolet and radiofrequency radiation of mobile phones on 3D reconstructed human skin in vitro. Int. J. Environ. Res. Public Health 17, 4401 (2020). https://doi.org/10.3390/ijerph17124401

Vijayalaxmi, C., Cao, Y., Scarfi, M.R.: Adaptive response in mammalian cells exposed to non-ionizing radiofrequency fields: a review and gaps in knowledge. Mutat. Res. 760, 36–45 (2014). https://doi.org/10.1016/j.mrrev.2014.02.002

Wang, H., Zhang, X.: Magnetic fields and reactive oxygen species. Int. J. Mol. Sci. 18, 2175 (2017). https://doi.org/10.3390/ijms18102175

Wang, L., Duan, Q., Wang, T., Ahmed, M., Zhang, N., Li, Y., Li, L., Yao, X.: Mitochondrial respiratory chain inhibitors involved in ROS production induced by acute high concentrations of iodide and the effects of SOD as a protective factor. Oxid. Med. Cell. Longevity 2015, 1–14 (2015). https://doi.org/10.1155/2015/217670

Wang, Y., Jiang, Z., Zhang, L., Zhang, Z., Liao, Y., Cai, P.: 3.5-GHz radiofrequency electromagnetic radiation promotes the development of *Drosophila melanogaster*. Environ. Pollut. 294, 118646 (2022). https://doi.org/10.1016/j.envpol.2021.118646

Wang, Y., Zhang, H., Zhang, Z., Sun, B., Tang, C., Zhang, L., Jiang, Z., Ding, B., Liao, Y., Cai, P.: Simulated mobile communication frequencies (3.5 GHz) emitted by a signal generator affects the sleep of *Drosophila melanogaster*. Environ. Pollut. 283, 117087 (2021). https://doi.org/10.1016/j.envpol.2021.117087

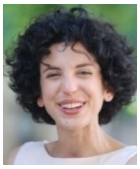
Xu, S., Chen, G., Chen, C., Sun, C., Zhang, D., Murbach, M., Kuster, N., Zeng, Q., Xu, Z.: Cell Type-dependent induction of DNA damage by 1800 MHz radiofrequency electromagnetic fields does not result in significant cellular dysfunctions. PLoS. ONE. 8, e54906 (2013). https://doi.org/10.1371/journal.pone.0054906

Yakymenko, I., Tsybulin, O., Sidorik, E., Henshel, D., Kyrylenko, O., Kyrylenko, S.: Oxidative mechanisms of biological activity of low-intensity radiofrequency radiation. Electromagn. Biol. Med. 35, 186–202 (2016). https://doi.org/10.3109/15368378.2015.1043557

Yang, H., Zhang, Y., Wu, X., Gan, P., Luo, X., Zhong, S., Zuo, W.: Effects of acute exposure to 3500 MHz (5G) radiofrequency electromagnetic radiation on anxiety-like behavior and the auditory cortex in guinea pigs. Bioelectromagnetics 43, 106–118 (2022). https://doi.org/10.1002/bem.22388

Zeni, O., Di Pietro, R., d'Ambrosio, G., Massa, R., Capri, M., Naarala, J., Juutilainen, J., Scarfi, M.R.: Formation of reactive oxygen species in L929 cells after exposure to 900 MHz RF radiation with and without co-exposure to 3-chloro-4-(dichloromethyl)-5-hydroxy-2(5H)-furanone. Radiat. Res. 167, 306–311 (2007). https://doi.org/10.1667/RR0595.1

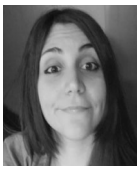
AUTHOR BIOGRAPHIES



Lorenza Patrignoni was born in 1990 in Tolentino, Italy. She received the master's degree in Chemistry and Technology of Drugs in 2015 from the University of Perugia, Perugia, Italy. She obtained its PhD in cellular and molecular physiopathology at the Ecole Pratique des Hautes Etudes of Paris (EPHE-PSL), in collaboration with the IMS laboratory of Bordeaux where she was engaged in the study of biological effects of radiofrequency on human cells.



Annabelle Hurtier is a Bordeaux INP biologist, engineer assistant, at the IMS laboratory. She is in charge of animal facility and is a specialist in animal welfare. She also performs cellular and molecular biology assays using qPCR, immunohistochemistry, and flow cytometry.



Rosa Orlacchio was born in Sapri, Italy. She received the MSc degree in Biomedical Engineering, (with honors), from "La Sapienza," University of Rome, Roma, Italy, and the PhD degree in Bioelectromagnetics from the Institute of Electronics and Telecommunications of Rennes (IETR), University of Rennes 1, Rennes, France, in 2014 and 2019, respectively. She is currently a Postdoctoral Researcher with the BioEM Team, XLIM Research Institute, CNRS, University of Limoges, Limoges, France. Her current research interests include the evaluation of the biological effects of nanosecond electric pulses (nsPEF) on cells, and thermal electromagnetic dosimetry and microdosimetry.



Alexandre Joushomme is a PhD student in bioelectromagnetics. His work is mainly focused on real-time assessment of environmental radiofrequency field effect on brain and skin live cells in vitro (holographic microscopy, impedence-metry, BRET).



Florence Poulletier de Gannes, PhD, is a CNRS research engineer at the IMS laboratory. Her research deals mainly with the adverse and beneficial biological effects of noninvasive electromagnetic fields funded by several national and foreign projects. She also works on EMF health risk assessment.



Philippe Lévêque (M'03) was born in Poitiers, France, in 1964. He received the PhD degree from the University of Limoges, Limoges, France, in 1994. In 1995, he joined CNRS. He is involved in the development of dosimetry and exposure setups for health-risk assessment in cooperation with biological and medical research groups. He is currently a senior scientist with CNRS and the group leader of Bioelectromagnetics Team with the XLIM Research Institute focusing on

1521186x, 2024, 3, Downloaded from https://onlinelibrary.wiley.com/doi/10.1002/bem.22495 by University Of British Columbia, Wiley Online Library on [10/10/2026]. See the Terms and Conditions (https://onlinelibrary.wiley.com/terms-and-conditions) on Wiley Online Library for rules of use; OA articles are governed by the applicable Creative Commons License

nanopulse application. His current research interest includes the scattering problems of electromagnetic waves, particularly in the time domain.



Delia Arnaud-Cormos (M'05) was born in Cugir, Romania, in 1978. She received the Diplôme d'Ingénieur degree from the Institute of Computer Science and Communication, Rennes, France, in 2002, and the master's and PhD degrees from INSA, Rennes, in 2003 and 2006, respectively. Since 2007, she has been with the Bioelectromagnetics Team, XLIM Institute, University of Limoges/CNRS, Limoges, France, as an associate professor. In 2012, she joined the Pulsed Power Group, University of Southern California (USC), Los Angeles, SC, USA, where she developed research with the Biological Applications Research Team. Since 2018, she has been a Junior Member with the Institut Universitaire de France (IUF), Paris, France, and a member of the International Bioelectrics Consortium. Her current research interests include nanosecond pulses/microwave exposure system setup and dosimetric characterization for bioelectromagnetic studies.



Hamid Reza Revzani performed his PhD at the INSERM U1035, where he has been trained in molecular and cell biology. His research there mainly focused on the role of DNA repair systems and reactive oxygen species (ROS) in keratinocytes responses to UVB irradiation. Getting a postdoctoral position in Prof. Bickers' lab at the University of Columbia, he then studied the relationships between DNA repair, ROS, and metabolic alterations during carcinogenesis using Xeroderma Pigmentosum type C (XPC) as model. Following his return to France, he continued his research on skin carcinogenesis, metabolism, DNA repair and redox signaling. He is co-director of the TRIO2 team at INSERM U1312/Bordeaux University. TRIO2 team studies phenotypic and genetic features, oncogenesis, metabolism flexibility, and microenvironment in order to develop a comprehensive, multidisciplinary, and integrative project on skin cancers.



Walid Mahfouf is an engineer within the TRIO2 team at the Bordeaux Institute of Oncology (INSERM U1312). Since 2011, his research has centered on investigating the effects of ultraviolet radiation on energy metabolism, reactive oxygen species, and DNA repair mechanisms, employing both in vitro and in vivo models.



André Garenne was born in Angoulême, France. He is a French pharmacist and neuroscientist. He obtained his PharmD from the University of Poitiers in 1996, bachelor's and master's degrees in computer science, and his PhD in biological and medical engineering from the University of Rennes 1 in 2003. He is currently a permanent associate professor at the University of Bordeaux, where he teaches computer science, biological modeling, and statistics. His current research focuses on the application of computational methods to the analysis and modeling of biological data.



Yann Percherancier is a cellular and molecular biochemist. During his PhD work at the Pasteur Institute (Paris, France), he studied the biochemistry of HIV-1 virus entry into T-lymphocytes, focusing on the role of specific lipid microdomains (also known as "lipid rafts") in this process. Y. P. continued his investigations as a postdoctoral researcher in the laboratory of Michel Bouvier (University of Montreal, Quebec, Canada), recognised worldwide as a gold standard in molecular pharmacology. In October 2005, he returned to France as a CNRS staff researcher, using the BRET technique to study various cellular process in real-time on living cells. In 2009, he moved to Bordeaux and joined the Bernard Veyret research group to work on bioelectromagnetism. His work now aims at deciphering EMF effects at the cellular and molecular level on living matter in real-time.



Isabelle Lagroye received the master degree in 1991, the PharmD degree and the PhD degree in life science in 1997, from the Bordeaux 2 University, France. After a postdoctoral position at the Radiation Oncology Center, Dr. Roti-Roti's laboratory, Saint-Louis, MO, USA, she has been doing research work with the Bioelectromagnetics Team, University of Bordeaux, Bordeaux, since 1999. She is a professor at the Ecole Pratique des Hautes Etudes, France. Her main research interests include the toxicological effects of non-invasive electromagnetic fields, investigating genotoxicity, apoptosis, protein expression, and stress markers in brain and skin models exposed to mobile phone signals. She is an author of 50 peer-reviewed papers and more than 20 invited conferences. She

1521186x, 2024, 3, Downloaded from https://onlinelibrary.wiley.com/doi/10.1002/bem.22495 by University Of British Columbia, Wiley Online Library on [10/10/2026]. See the Terms and Conditions (https://onlinelibrary.wiley.com/terms-and-conditions) on Wiley Online Library for rules of use; OA articles are governed by the applicable Creative Commons License

was part of the Static and ELF Fields EHC Task Groups at WHO, and participant in technical consultation for WHO RF research agenda in 2010. Dr. Lagroye is a member of the BioElectroMagnetics Society.

SUPPORTING INFORMATION

Additional supporting information can be found online in the Supporting Information section at the end of this article.

How to cite this article: Patrignoni L., Hurtier A., Orlacchio R., Joushomme A., de Gannes F.P., Lévêque P., Arnaud-Cormos D., Revzani H.R., Mahfouf W., Garenne A., Percherancier Y., Lagroye I.: Evaluation of mitochondrial stress following ultraviolet radiation and 5G radiofrequency field exposure in human skin cells. Bioelectromagnetics, 45, 110–129 (2024)

1521186x, 2024, 3, Downloaded from https://onlinelibrary.wiley.com/doi/10.1002/bem.22495 by University Of British Columbia, Wiley Online Library on [10/10/2026]. See the Terms and Conditions (https://onlinelibrary.wiley.com/terms-and-conditions) on Wiley Online Library for rules of use; OA articles are governed by the applicable Creative Commons License